

## RESEARCH ARTICLE

# Group 1 CD1-restricted T cells contribute to control of systemic *Staphylococcus aureus* infection

Lavanya Visvabharathy<sup>1</sup>, Samantha Genardi<sup>1</sup>, Liang Cao<sup>1</sup>, Ying He<sup>1</sup>, Francis Alonzo, III<sup>2</sup>, Evgeny Berdyshev<sup>3</sup>, Chyung-Ru Wang<sup>1\*</sup>

**1** Department of Microbiology and Immunology, Feinberg School of Medicine, Northwestern University, Chicago, United States of America, **2** Department of Microbiology and Immunology, Stritch School of Medicine, Loyola University, Maywood, United States of America, **3** Department of Medicine, National Jewish Health, Denver, United States of America

\* [chyung-ru-wang@northwestern.edu](mailto:chyung-ru-wang@northwestern.edu)



## OPEN ACCESS

**Citation:** Visvabharathy L, Genardi S, Cao L, He Y, Alonzo F, III, Berdyshev E, et al. (2020) Group 1 CD1-restricted T cells contribute to control of systemic *Staphylococcus aureus* infection. PLoS Pathog 16(4): e1008443. <https://doi.org/10.1371/journal.ppat.1008443>

**Editor:** David M. Lewinsohn, Portland VA Medical Center, Oregon Health and Science University, UNITED STATES

**Received:** September 25, 2019

**Accepted:** February 28, 2020

**Published:** April 28, 2020

**Copyright:** © 2020 Visvabharathy et al. This is an open access article distributed under the terms of the [Creative Commons Attribution License](https://creativecommons.org/licenses/by/4.0/), which permits unrestricted use, distribution, and reproduction in any medium, provided the original author and source are credited.

**Data Availability Statement:** All relevant data are within the manuscript and its Supporting Information files.

**Funding:** This work is supported by NIH R01 grant AI057460 (to CRW) and T32 AI007476 to (LV). The funders had no role in study design, data collection and analysis, decision to publish, or preparation of the manuscript.

**Competing interests:** The authors have declared that no competing interests exist.

## Abstract

*Staphylococcus aureus* (SA) is the causative agent of both skin/soft tissue infections as well as invasive bloodstream infections. Though vaccines have been developed to target both humoral and T cell-mediated immune responses against SA, they have largely failed due to lack of protective efficacy. Group 1 CD1-restricted T cells recognize lipid rather than peptide antigens. Previously found to recognize lipids derived from cell wall of *Mycobacterium tuberculosis* (Mtb), these cells were associated with protection against Mtb infection in humans. Using a transgenic mouse model expressing human group 1 CD1 molecules (hCD1Tg), we demonstrate that group 1 CD1-restricted T cells can recognize SA-derived lipids in both immunization and infection settings. Systemic infection of hCD1Tg mice showed that SA-specific group 1 CD1-restricted T cell response peaked at 10 days post-infection, and hCD1Tg mice displayed significantly decreased kidney pathology at this time point compared with WT control mice. Immunodominant SA lipid antigens recognized by group 1 CD1-restricted T cells were comprised mainly of cardiolipin and phosphatidyl glycerol, with little contribution from lysyl-phosphatidyl glycerol which is a unique bacterial lipid not present in mammals. Group 1 CD1-restricted T cell lines specific for SA lipids also conferred protection against SA infection in the kidney after adoptive transfer. They were further able to effectively control SA replication in vitro through direct antigen presentation by group 1 CD1-expressing BMDCs. Together, our data demonstrate a previously unknown role for group 1 CD1-restricted SA lipid-specific T cells in the control of systemic MRSA infection.

## Author summary

The bacterial pathogen *Staphylococcus aureus* (SA) is the cause of skin as well as invasive bloodstream infections, both in hospital and community settings. Efforts to develop preventative vaccines have been unsuccessful so far despite focusing on stimulating both B cell and T cell responses against SA. However, the unconventional group 1 CD1-restricted

lipid-reactive T cell subset has never been studied in the context of systemic SA infection, and investigating their contribution to SA host defense could be fruitful in anti-SA vaccine design. Using a mouse model expressing group 1 CD1 molecules, we show that these T cells recognize and are activated by SA lipids during immunization and infection. The presence of group 1 CD1-restricted T cells decrease kidney inflammation in mice, and transfer of these cells into mice before SA infection results in ~10,000-fold decreases in kidney bacterial burdens. Together, our data demonstrate that activation of the group 1 CD1-restricted T cell response may be a promising avenue to investigate in the development of anti-SA vaccines.

## Introduction

*Staphylococcus aureus* (SA) is one of the most frequently isolated pathogens associated with nosocomial infections [1]. SA infection commonly manifests in many different organ niches, including skin/soft tissue infections, respiratory tract infections, pneumonia, and endocarditis [2]. SA also causes invasive sepsis leading to septic shock and multiple organ failure [3–6]. Antibiotic treatment of SA is complicated by the prevalence of methicillin resistant SA (MRSA) strains in hospitals and increasingly in community settings [3] [7], resulting in patient mortality rates of 16.6% in 2017 in addition to elevated healthcare costs [8–10]. Multiple vaccine strategies have been employed with limited efficacy against recurrent infection [11–13].

As an extracellular pathogen, historically it was thought that the antibody response was critical to immunity against SA [14, 15]. However, the contribution of T cells to anti-SA immunity is gradually becoming appreciated. One study identified a CD4<sup>+</sup> T cell epitope from the SA heme-uptake protein IsdB able to induce proliferation and IFN- $\gamma$  and IL-17 secretion from T cells [16]. Another group identified the epitope M8 derived from manganese transport protein C (MntC) to induce proliferation and IL-17 secretion from CD4<sup>+</sup> T cells in immunized BALB/c mice [17]. Studies in humans without documented prior infection with SA showed that healthy people possess a significant pool of SA Ag-specific CD4<sup>+</sup> memory T cells [18], and mouse studies have linked expansion of IL-17-producing  $\gamma\delta$  T cells with protection against SA [19]. Additionally, patients with hyper-IgE syndrome who lack the ability for Th17 CD4<sup>+</sup> T cell differentiation are highly susceptible to SA skin infections [20], and HIV<sup>+</sup> patients are more susceptible to MRSA skin infections possibly due to decreased IFN- $\gamma$  production from SA Ag-specific CD4<sup>+</sup> T cells [21]. Intriguingly, recent studies have found a clonal V $\gamma$ 6<sup>+</sup>V $\delta$ 4<sup>+</sup> T cell subset secreting IL-17 to be crucial for protective immunity against SA skin infection in mice [22]. Despite data showing the importance of conventional CD4<sup>+</sup> T cells and  $\gamma\delta$  T cells to defense against SA, the role of lipid antigen-specific group 1 CD1-restricted T cells remains unexplored.

CD1 molecules are structurally similar to MHC-I molecules and present self- and microbial-derived lipids to T cells [23]. Three major groups of CD1 have been identified in humans: group 1 CD1 (CD1a, -b, and -c), group 2 CD1 (CD1d), and group 3 CD1 (CD1e; aids in loading complex lipids onto CD1b molecules) [24, 25]. CD1d is the restriction element for type I and type II NKT cells, innate-like T cells which have been shown to play a role in defense against various microbial infections [26–28]. NKT cells exhibit pre-activated phenotype and are rapidly mobilized to fight microbial infections [29]. Studies have demonstrated that type I NKT cells (or iNKT cells) can be activated by both antigen-specific and cytokine-driven mechanisms, for example through interaction of *Salmonella Typhimurium*-derived LPS with TLRs on antigen presenting cells, inducing production of IL-12 [30]. Additionally, activation of type

II NKT cells has been shown to protect against SA-mediated sepsis in mouse models of infection [31]. However, though both group 1 and group 2 CD1-restricted T cells are activated by lipid antigens, it is unknown whether the kinetics and function of group 1 CD1-restricted T cell responses to SA mimic the innate-like responses seen with NKT cells. Though mice only express CD1d, our lab has developed a transgenic mouse model (hCD1Tg) expressing human group 1 and group 3 CD1 molecules in a tissue specific, physiologically relevant manner [32]. To date, studies have shown that group 1 CD1-restricted T cells can recognize and respond to mycobacterial lipid antigens during infection in hCD1Tg mice [32, 33]. In addition, Mtb lipid-specific group 1 CD1-restricted T cells contribute to anti-Mtb immunity through increased IFN- $\gamma$  cytokine secretion [23, 33, 34], and Mtb patients have higher numbers of these T cells in circulation [35]. While Group 1 CD1-restricted microbial antigens identified thus far have mainly been of mycobacterial origin [25, 34, 36], CD1 molecules may bind lipid antigens from a broad range of pathogens because their antigen binding grooves can accommodate a variety of lipid species [37, 38]. Indeed, humans have CD1b-restricted T cells that recognize lipids from *Staphylococcus aureus*, *Brucella melitensis*, *Salmonella Typhimurium*, and *Borrelia burgdorferi* [39, 40].

To determine how group 1 CD1-restricted T cell dynamics and function change in response to different infectious agents, we selected SA as a model pathogen. SA contains microbial lipid moieties [41] sharing several common features with other group 1 CD1-binding antigens. Indeed, one recent study showed that CD1b dextramers loaded with phosphatidylglycerol (PG) from SA can identify and cross-react with autoreactive group 1 CD1-restricted T cells in humans [39]. Based on these studies, it is important to identify whether group 1 CD1-restricted T cells play a similar role in anti-SA immunity in vivo.

Using in vivo models of systemic SA infection in hCD1Tg mice, we found that group 1 CD1-restricted T cell responses against SA lipids can be detected in both immunization and infection settings. The kinetics of group 1 CD1-restricted T cell activation more closely resembled conventional T cell rather than NKT cell activation patterns, and hCD1Tg mice trended towards decreased kidney CFU burden and pathology compared with Tg- WT littermate controls. Fractionation of SA lipids revealed cardiolipins and polar phospholipids to be immunodominant lipid moieties recognized by group 1 CD1-restricted T cells. Furthermore, T cell lines specific for these lipids were protective against SA infection in hCD1Tg mice. SA killing experiments with group 1 CD1-restricted T cell lines specific for SA lipids also resulted in efficient CFU control in vitro. These findings demonstrate that group 1 CD1-restricted T cells can respond to SA lipids and that they contribute to protection against SA infection.

## Results

### Immunization of hCD1Tg mice with SA lipids activates group 1 CD1-restricted T cells

We have previously shown that both infection with Mtb and immunization with Mtb lipids elicit group 1 CD1-restricted T cell responses in hCD1Tg mice. However, it was unknown whether group 1 CD1-restricted T cells could respond to SA lipids in hCD1Tg mice. As a proof of principle, we immunized hCD1Tg mice intraperitoneally with BMDCs expressing CD1b and CD1c (78<sup>+</sup>Tg, or Tg<sup>+</sup> BMDCs) coated with total SA lipid extract from USA300 LAC. At 7 days post immunization, lymphocytes from peripheral lymph nodes of immunized mice were stimulated ex vivo with Tg<sup>-</sup> or Tg<sup>+</sup> BMDC pulsed or unpulsed with SA lipids, and IFN- $\gamma$ -producing cells were quantified by ELISPOT assays. A significantly higher number of IFN- $\gamma$ -producing cells were detected when stimulated with SA lipid-pulsed Tg<sup>+</sup> DC compared to stimulation with SA lipid-pulsed Tg<sup>-</sup> DCs or unpulsed DCs. This data indicate that SA lipid

immunization can induce group 1 CD1-restricted SA lipid-specific T cell responses in hCD1Tg mice (Fig 1). Further, addition of CD1b and CD1c blocking antibodies showed that the majority of the group 1 CD1 response to SA lipids was CD1b-restricted, with a moderate contribution from CD1c-restricted T cells. Naïve, unimmunized mice also displayed a group 1 CD1-restricted T cell response to SA lipids which was also predominantly CD1b-restricted, though the magnitude of the response was much lower than what was seen in immunized mice. This suggested that a portion of the CD1b-restricted T cell response to SA lipid was due to activation of cross-reactive CD1b-autoreactive T cells.

### Group 1 CD1-restricted T cell responses directed against SA lipids can be detected during systemic SA infection in hCD1Tg mice

Based on data showing that immunization with SA lipids induces group 1 CD1-restricted T cell responses, we infected hCD1Tg mice with SA to determine if infection induced similar SA lipid-specific responses. hCD1Tg mice expressing CD1b and CD1c molecules (78<sup>+</sup>Tg mice) were infected with MRSA strain USA300 LAC, an isolate that frequently causes community-acquired skin and soft-tissue infections as well as systemic infections [42]. Mice were injected with 5x10<sup>6</sup> CFU via tail vein and euthanized at 10 days post-infection. Lymphocytes were isolated from cervical, axillary, inguinal, renal, and mesenteric lymph nodes and cultured together with Tg<sup>-</sup> or Tg<sup>+</sup> BMDCs pulsed or unpulsed with SA lipids. This experiment was also conducted in hCD1Tg mice expressing CD1a, -b, and -c (64<sup>+</sup>Tg mice) and we obtained a similar magnitude of response, though there was some contribution of autoreactive CD1a-restricted T cells that was not observed in 78<sup>+</sup>Tg mice (S1 Fig). However, 78<sup>+</sup>Tg mice were used in subsequent experiments due to their ability to breed more effectively. Group 1 CD1-restricted T cells produced IL-17 and IFN- $\gamma$  in response to total SA lipids in ELISPOT assays (Fig 2A). In order to confirm these responses to be SA lipid-specific and independent of non-specific superantigen-mediated T cell activation, the experiment was repeated in hCD1Tg MHC-II<sup>-/-</sup> mice (Fig 2B), with similar results. We also demonstrated that the group 1 CD1-restricted T cell response to SA lipids were not affected by the presence of NKT cells, as hCD1Tg CD1d<sup>-/-</sup> mice had similar levels of IFN- $\gamma$  and IL-17A production as hCD1Tg WT mice (Fig 2C). In contrast to the lymph nodes, lymphocytes isolated from the spleen did not show measurable group 1 CD1-restricted SA lipid-specific responses, possibly due to the expansion of myeloid-derived suppressor cells that can limit T cell activation [43; data not shown]. We additionally determined whether SA lipid-specific group 1 CD1-restricted T cell responses were present in the kidney because it is the primary reservoir for SA during systemic infection [44]. We were unable to reliably detect these responses in the kidney at 10 days post-infection (S2 Fig), and therefore the remainder of the data focuses on group 1 CD1-restricted T cell responses in the lymph nodes. Together, these data show that group 1 CD1-restricted T cells can recognize and respond to SA lipids during systemic infection with SA.

### Group 1 CD1-restricted T cell response to SA peaks at 10 days post-infection

To determine the kinetics of the group 1 CD1-restricted T cell response during SA infection, hCD1Tg mice were infected i.v. with SA and sacrificed at 7, 10, and 21 days post-infection. The group 1 CD1-restricted T cell response to SA lipids peaked at 10 days, and had waned by 21 days post-infection (Fig 3A). This mirrored the activation pattern of conventional T cells, as reflected by the upregulation of CD69 expression on CD4<sup>+</sup> and CD8<sup>+</sup> T cells (S3A Fig). However, the peak of the group 1 CD1 response was not correlated with significant upregulation of CD1b or CD1c on APCs (e.g. B cells, macrophages, and dendritic cells) in lymph nodes of

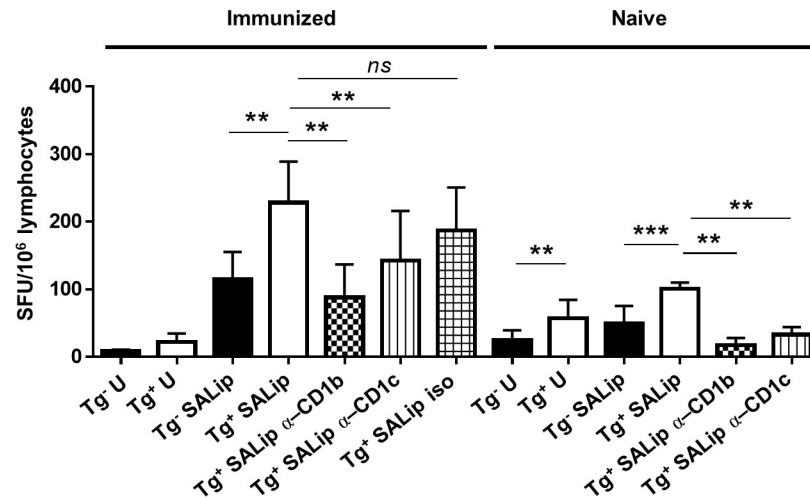


**Fig 1. Group 1 CD1-restricted T cell responses against SA lipids are detected after immunization of hCD1Tg mice.** hCD1Tg mice expressing CD1b and CD1c were immunized i.p. with Tg<sup>+</sup> BMDCs coated with total SA lipid extract. Lymphocytes from pooled peripheral lymph nodes (cervical, axillary, inguinal, and mesenteric) were isolated at day 7 from immunized and naïve hCD1Tg mice. Lymphocytes were assayed for IFN- $\gamma$  production via ELISPOT using Tg<sup>-</sup> or Tg<sup>+</sup> BMDCs  $\pm$  total SA lipid as stimulators. Anti-CD1b or -CD1c blocking antibody or isotype control was added as indicated. Data is representative of 2 independent experiments with  $n = 1$  (naïve) or 5 (immunized) mice each plated in duplicate. \*\* $p < 0.01$  using two-way ANOVA with Tukey's multiple comparisons posttest.

<https://doi.org/10.1371/journal.ppat.1008443.g001>

infected mice at 10dpi (S3B and S3C Fig). As the phenotypic characteristics of group 1 CD1-restricted T cells induced during SA infection are unknown, we further determined their co-receptor usage in SA-infected hCD1Tg mice. Lymphocytes from lymph nodes of infected mice were stimulated with Tg<sup>-</sup> or Tg<sup>+</sup> BMDCs pulsed with SA lipid antigen and intracellular cytokine staining for IL-17A was performed to identify SA lipid-specific group 1 CD1-restricted T cells (Fig 3B). We found that most of group 1 CD1-restricted SA lipid-specific T cells express either CD4 or CD8 co-receptors (Fig 3B, bottom right).

We next investigated whether the presence of group 1 CD1-restricted T cells conferred protection against systemic SA infection. Interestingly, there was a trend toward decreased CFU in kidneys of hCD1Tg mice compared with Tg<sup>-</sup> littermate controls at 10 days post-infection (Fig 3C), which correlated with the peak of the group 1 CD1-restricted response to SA lipids. In addition, hCD1Tg mice exhibited significantly decreased kidney pathology compared with Tg<sup>-</sup> littermate controls. Hematoxylin and eosin staining performed on infected hCD1Tg and Tg<sup>-</sup> kidneys at 10 days post-infection showed that Tg<sup>-</sup> kidneys displayed significantly larger areas of abscesses and inflammation (Fig 3D). Immunofluorescence on whole kidney sections further showed that abscesses were more disorganized in Tg<sup>-</sup> (WT) mice compared with hCD1Tg mice at the same time point (Fig 3E). This trend toward enhanced disorganization in neutrophil recruitment and abscess formation occurred across most of the Tg<sup>-</sup> kidneys examined (S4 Fig). In contrast, Tg<sup>+</sup> kidneys had small, defined abscesses and foci of inflammation which limited the total area of kidney damage.

### Fractionation of SA lipids reveals immunodominant phospholipid components

Having shown that SA infection can elicit SA lipid-specific group 1 CD1-restricted T cell responses, we next sought to identify immunodominant SA lipid antigens recognized during SA infection. Total SA lipids were isolated from lysostaphin-treated USA300 LAC in order to

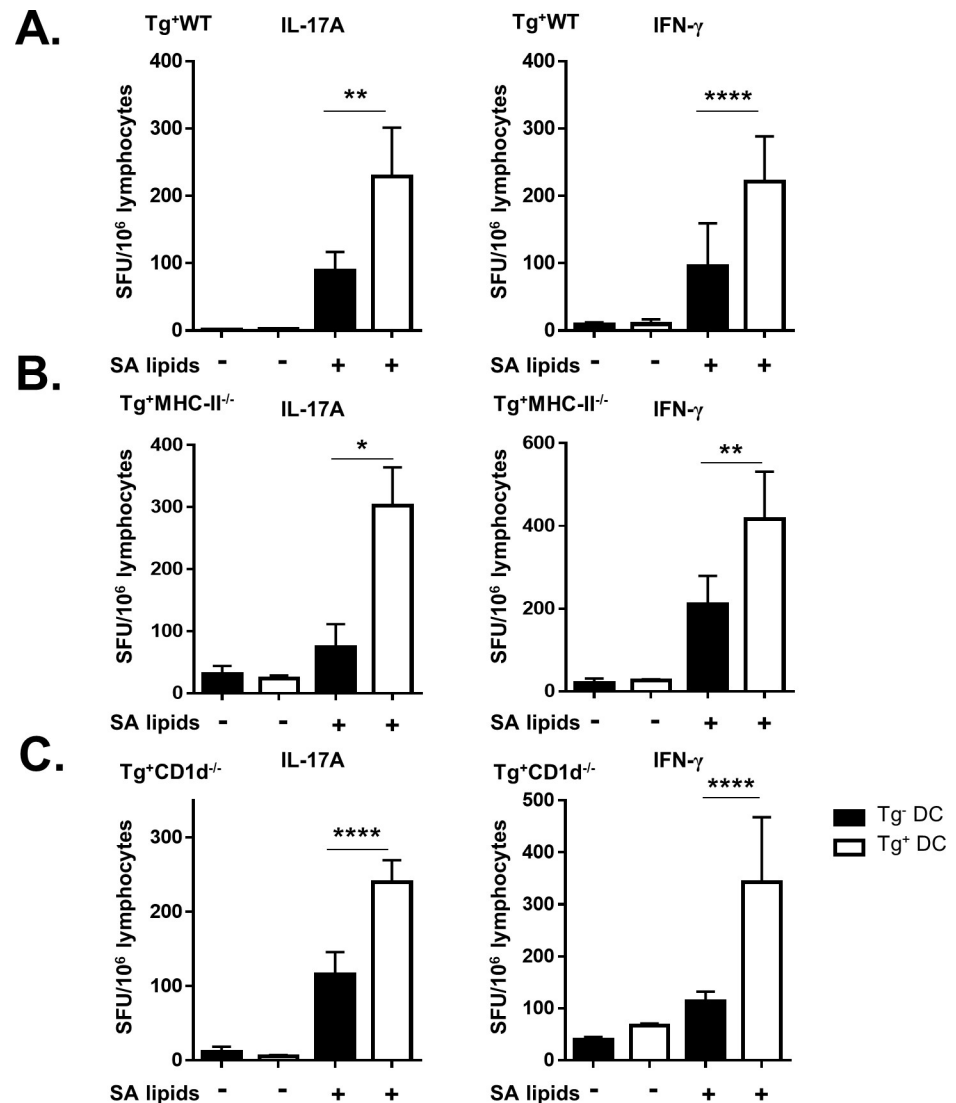


**Fig 2. SA lipid-specific group 1 CD1-restricted T cell responses occur during systemic infection with MRSA.** hCD1Tg (A) or hCD1Tg MHC-II<sup>-/-</sup> (B) or hCD1Tg CD1d<sup>-/-</sup> (C) mice were infected with  $5 \times 10^6$  CFU of USA300 MRSA via tail vein. At 10 days post-infection, lymphocytes from lymph nodes of indicated mice were stimulated with Tg<sup>-</sup> or Tg<sup>+</sup> BMDCs  $\pm$  total SA lipid and IL-17A and IFN- $\gamma$ -secreting cells were quantified by ELISPOT. Data representative of 3–5 independent experiments with  $n = 4$ –5 mice per group. \* $p < 0.05$ , \*\* $p < 0.01$ , \*\*\*\* $p < 0.0001$  using two-way ANOVA with Tukey's multiple comparisons posttest.

<https://doi.org/10.1371/journal.ppat.1008443.g002>

eliminate peptidoglycan contamination and limit purification to membrane-associated bacterial lipids. Lipids were fractionated using silica gel column chromatography and sequential elution of neutral lipids by chloroform, glycolipids by acetone, column re-equilibration in chloroform and by increasing methanol proportion in chloroform to elute more polar lipids. Lipids were separated into 8 discrete fractions (Fig 4A) containing neutral lipids, moderately polar lipids, and polar phospholipids. Fraction 3 contained cardiolipin species with saturated acyl chains of various chain lengths (S5A Fig). PG-enriched fractions 6–8 consisted of PG species with acyl chains lengths identical to cardiolipin in Fraction 3 (S5A Fig), but PG and lysyl-PG were present in different proportions in each fraction, causing the fractions to elute in different solvent compositions (S5B Fig). However, Fraction 8 did contain a PG moiety of unique

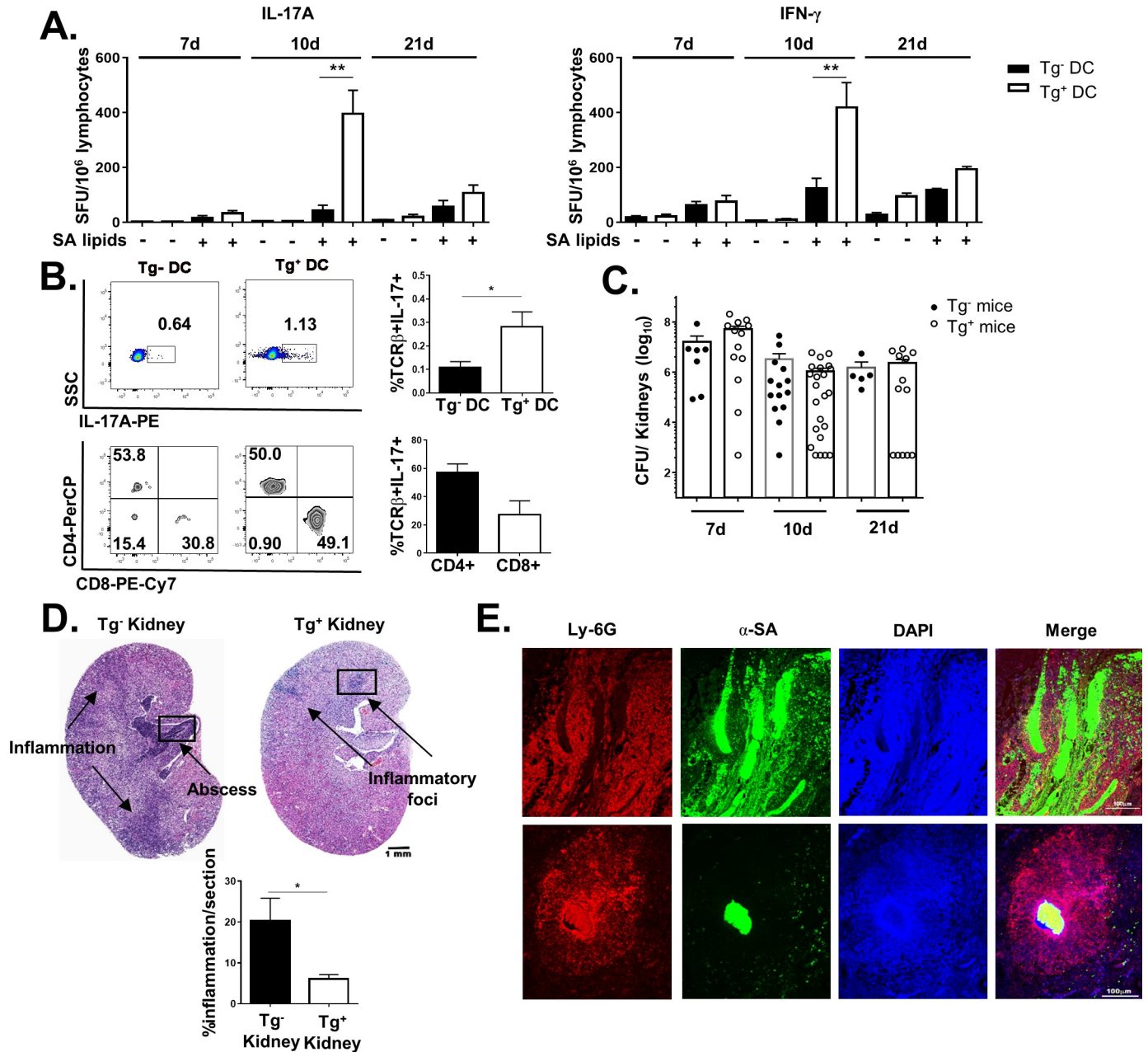


**Fig 3. SA lipid-specific group 1 CD1-restricted T cell response helps to contain kidney inflammation.** (A) Lymphocytes from lymph nodes of hCD1Tg mice were isolated at 7, 10, and 21 days post-infection. Frequency of IL-17A and IFN- $\gamma$ -secreting cells were quantified by ELISPOT using Tg<sup>-</sup> and Tg<sup>+</sup> BMDC  $\pm$  total SA lipids as stimulators. Data are combined from 4 independent experiments with n = 4–6 mice per time point. \*\* p<0.01 using 1-way ANOVA with Tukey’s posttest. (B) Enriched  $\alpha\beta$  T cells from SA-infected hCD1Tg mice at day 10 post-infection were stimulated with SA lipid pulsed Tg<sup>-</sup> or Tg<sup>+</sup> BMDCs. Intracellular cytokine staining for IL-17A was then performed along with surface FACS staining to determine the expression of CD4 and CD8 on SA lipid-specific group 1 CD1 T cells. Data representative of 3 independent experiments with n = 5–6 mice per experiment. \*p<0.05 using two-tailed Student’s t test. (C) CFU enumeration of SA in kidneys of hCD1Tg and Tg<sup>-</sup> mice at various times post-infection. Data pooled from 5 independent experiments. (D) Hematoxylin and eosin staining of hCD1Tg<sup>+</sup> and Tg<sup>-</sup> kidney sections at 10 days post-infection. Black boxes denote area shown in Figure E. Bar graphs quantify percentage of kidney tissue associated with inflammation. Data representative of 2 independent experiments with n = 3–6 mice per group. \*p<0.05 using two-tailed Student’s t test. (E) Immunofluorescent staining was performed on paraffin-embedded kidney sections isolated from hCD1Tg mice at 10 days post-infection. Neutrophils: anti-Ly-6G, red; SA: anti-SA, green. Data representative of 2 independent experiments with n = 3–5 mice/group.

<https://doi.org/10.1371/journal.ppat.1008443.g003>

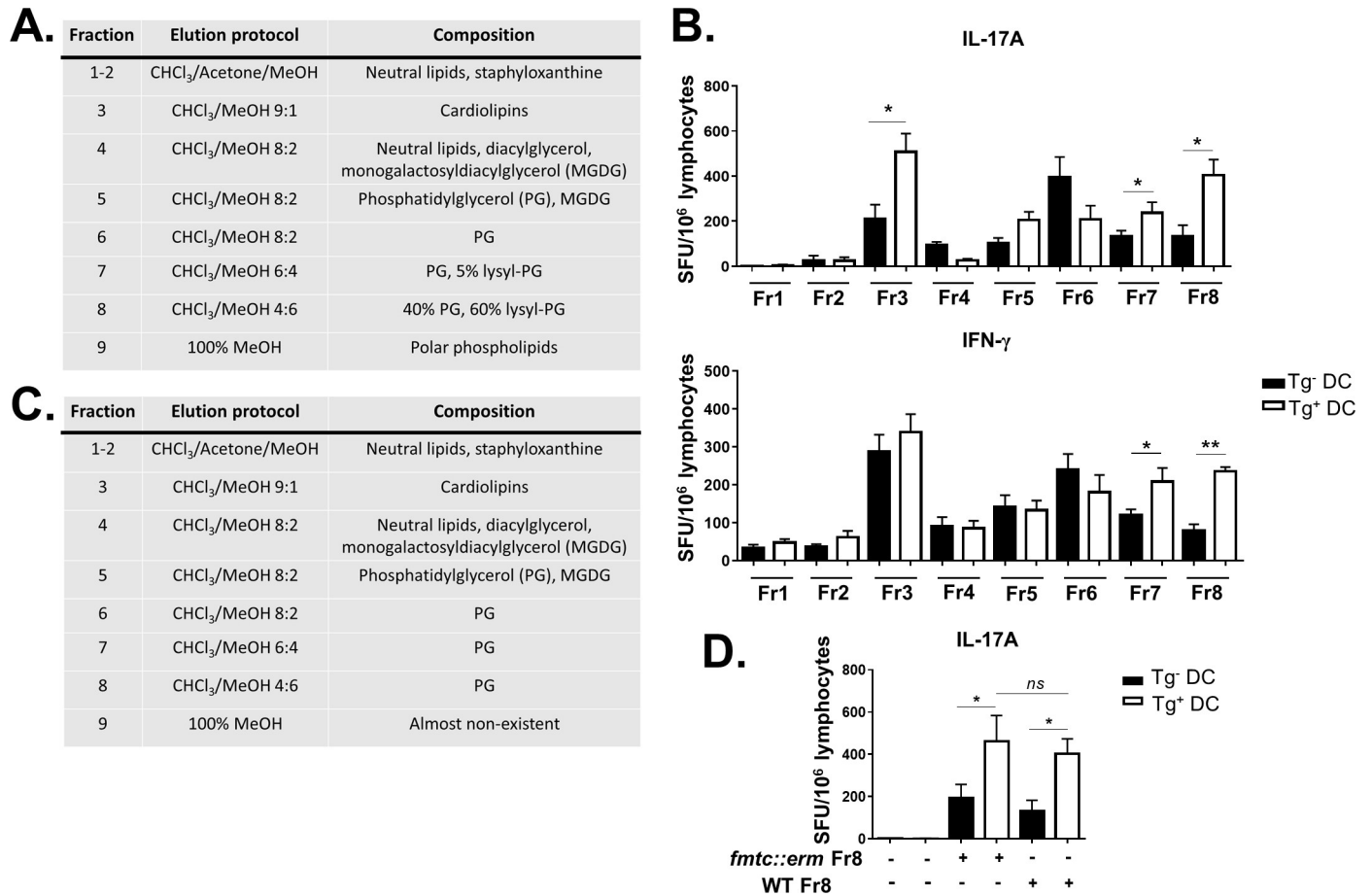


**Fig 4. Phosphatidyl glycerol moieties are immunodominant SA lipids recognized by group 1 CD1-restricted T cells.** (A) Lipid composition of various fractions isolated from SA using CHCl<sub>3</sub>-MeOH step gradients. (B) Lymphocytes from pooled peripheral lymph nodes were isolated from SA-infected hCD1Tg mice at 10 days post-infection. Frequency of IL-17A and IFN- $\gamma$ -producing T cells to various SA lipid fractions were quantitated by ELISPOT. Data representative of 2 independent experiments with n = 5–7 mice per experiment. (C) Table showing lipid composition of various fractions isolated from *fmtC::erm* USA300 strain lacking lysyl-PG. (D) Lymphocytes from hCD1Tg mice were stimulated with Tg<sup>-</sup> or Tg<sup>+</sup> BMDCs pulsed with Fr 8 from WT or the *fmtC::erm* mutant and assayed for IL-17A production as above. \*p<0.05; \*\*p<0.01 using 2-way ANOVA with Tukey's posttest.

<https://doi.org/10.1371/journal.ppat.1008443.g004>

acyl chain length (21:0/15:0; S5A Fig). IFN- $\gamma$  and IL-17 ELISPOT assays readily detected group 1 CD1-restricted T cell responses directed toward fractions 7 & 8 (Fr7, Fr8; phosphatidyl glycerol-enriched) at 10 days post-infection (Fig 4B). Interestingly, group 1 CD1-restricted T cells also recognized lipids from fraction 3 (Fr3; cardiolipin-enriched), but this fraction selectively induced IL-17 and not IFN- $\gamma$  production in a group 1 CD1-dependent manner.

Mass spectrometry analysis showed that Fr8 contained a mixture of phosphatidyl glycerol (PG) and lysyl-phosphatidyl glycerol (lysyl-PG) species. We originally hypothesized that lysyl-PG may play a dominant role in activating group 1 CD1-restricted T cells because lysyl-PG is unique to bacteria [45] while PG species are found in bacterial membrane as well as mitochondrial membranes in mammalian cells [46]. To test this, we generated a *fmtC::erm* SA mutant that is capable of synthesizing PG but is unable to lysylate it to form lysyl-PG [45]. The absence of lysyl-PG species in total lipid extract from *fmtC::erm* was confirmed by mass spectrometry (S6 Fig). Lipids from the *fmtC::erm* mutant were fractionated (Fig 4C) and tested in a IL-17 ELISPOT assay using lymphocytes from infected hCD1Tg mice at 10 days post-infection. Contrary to our hypothesis, group 1 CD1-restricted T cells retained their reactivity to Fr8 from the

*fntC::erm* strain (Fig 4D), suggesting that PG but not lysyl-PG species are the immunodominant lipids they recognize. Interestingly, no group 1 CD1-restricted T cell responses were detected towards purified mammalian 16:0–18:1 cardiolipin or 18:0 PG (S7 Fig), suggesting that SA-derived cardiolipin and PG species uniquely activate these T cells during systemic SA infection.

### Group 1 CD1-restricted T cell lines specific for SA lipids are polyfunctional and recognize multiple lipid species

In order to further probe the function of SA lipid-specific group 1 CD1-restricted T cells, we generated group 1 CD1-restricted SA lipid-specific T cell lines from lymphocytes of infected hCD1Tg mice by re-stimulating them weekly with Tg<sup>+</sup> BMDCs pulsed with total SA lipids. A panel of group 1 CD1-restricted T cell lines were generated and we chose to focus on 3 cell lines in particular due to their specificity and ability to produce multiple cytokines. All 3 T cell lines were reactive to SA lipids and could produce IFN- $\gamma$  as well as either IL-17 or TNF- $\alpha$  (Fig 5A). These responses were truly SA lipid-specific and Tg-dependent, as SA lipid pulsing did not affect BMDC maturation or IL-6 production differentially between Tg<sup>-</sup> and Tg<sup>+</sup> BMDCs alone (S8 Fig). They also showed different immunodominance hierarchies in response to SA lipids (Fig 5B). All 3 cell lines were poly-functional and could produce TNF- $\alpha$ , IFN- $\gamma$ , and granzyme B in response to PMA and Ionomycin stimulation; cell line 5–7 was unique in that it also produced IL-17 (Fig 5C). These group 1 CD1-restricted T cell lines were also poly-functional in response to SA lipids (Fig 5D). Each T cell line was double negative (possibly due to loss of co-receptor after long term primary T cell culture) used different V $\beta$  chains, and most were CD1b-restricted (Fig 5E). Though all 3 cell lines used the V $\alpha$ 11 chain, sequence analysis demonstrated that J region rearrangements were different among them (Fig 5E). Finally, cytokine production from each cell line was likely dependent upon TCR activation by group 1 CD1 molecules, as IFN- $\gamma$  production was retained when T cells were simulated by APCs lacking the critical innate immune signaling adaptor protein MyD88 (S9 Fig).

### Adoptive transfer of CD1b-restricted T cells specific for SA lipids protects against SA infection in hCD1Tg mice

Adoptive transfer of mycolic acid-specific CD1b-restricted T cells have been shown to confer protection against Mtb infection in hCD1Tg mice [33]. To test whether SA lipid-specific CD1b-restricted T cells were protective against SA infection, hCD1Tg mice and sex-matched Tg<sup>-</sup> littermate controls were injected with either PBS or 2x10<sup>6</sup> cells of T cell line 51 via tail vein. Mice were infected with SA i.v. 24h later and euthanized at 4 days post-infection. hCD1Tg mice that received cell line 51 (Tg<sup>+</sup> AT) had significantly lower bacterial burden (~4 log) in the kidneys compared with either hCD1Tg mice that only received PBS (Tg<sup>+</sup> no AT) or Tg<sup>-</sup> mice that had also received cell line 51 (Tg<sup>-</sup> AT) (Fig 6A). Consistent with this, the Tg<sup>+</sup> AT group had significantly fewer infiltrating immune cells in the kidney than the other groups (Fig 6B), possibly due to lower bacterial burdens in the organ. Significantly, the adoptively transferred cell line 51 (identified using the labeling reagent CellTrace) were found in greater quantity in the livers of hCD1Tg mice than in Tg<sup>-</sup> recipient mice (Fig 6C and 6D), suggesting the presence of group 1 CD1 molecules is crucial for their activation in vivo. In addition, conventional CD4<sup>+</sup> T cells in the Tg<sup>+</sup> AT group produced significantly more IFN- $\gamma$  than the other two groups, and CD8 T cells were similarly more activated in the lymph nodes than the other groups (Fig 6E and 6F). This data suggests that activation of CD1b-restricted SA lipid-specific T cells can lead to conventional T cell transactivation during SA infection.

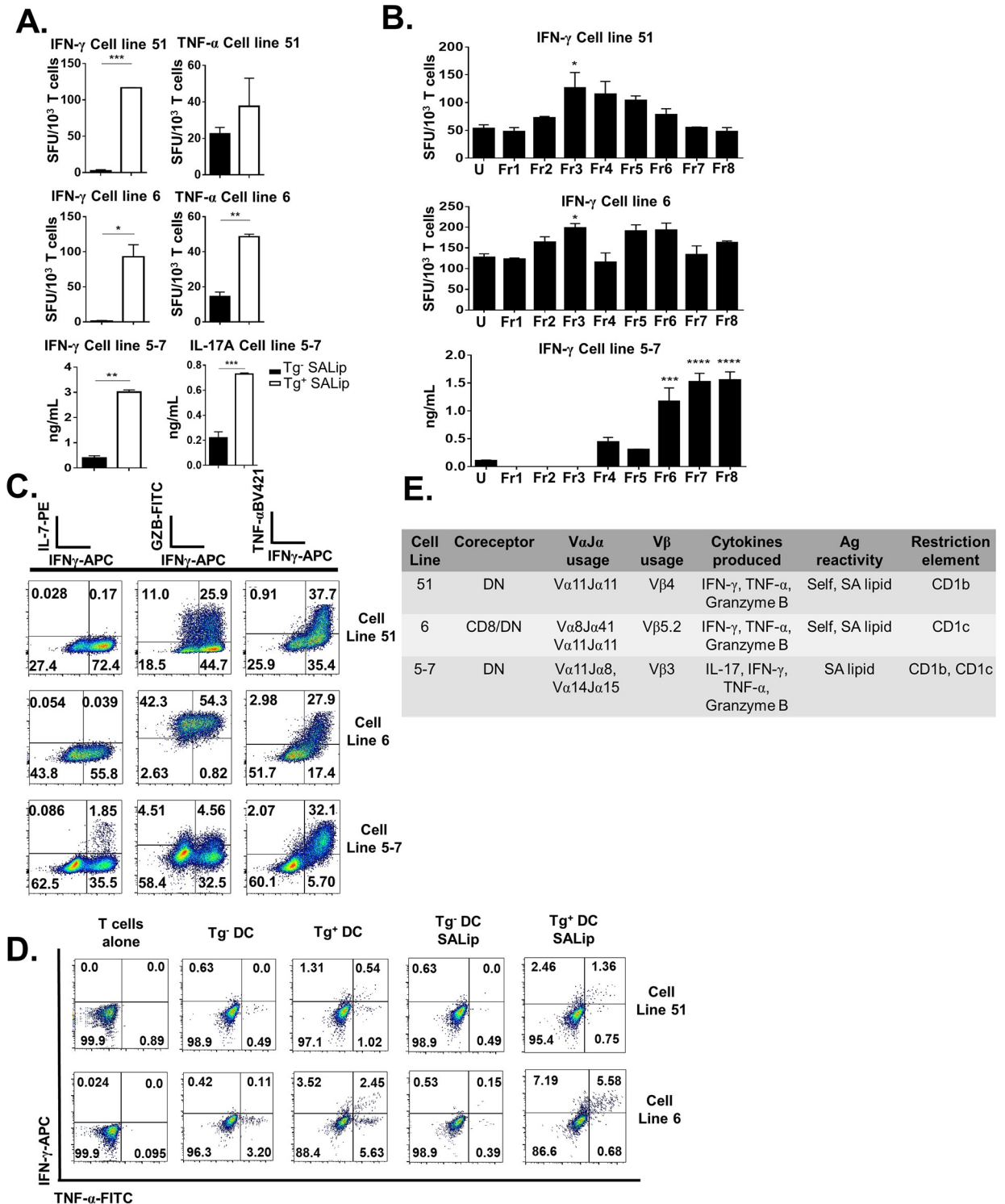


**Fig 5. Group 1 CD1-restricted T cell lines respond to polar lipids and phosphatidyl glycerols from SA.** T cell lines 51, 6 and 5–7 were derived from splenocytes of SA-infected hCD1Tg mice. (A) T cell lines were cultured with SA lipid-pulsed Tg<sup>-</sup> or Tg<sup>+</sup> BMDCs and assayed for IFN- $\gamma$ , TNF- $\alpha$ , or IL-17 production by ELISA or ELISPOT as indicated. (B) T cell lines 51, 6, and 5–7 mainly recognize polar lipids and phospholipids from SA. T cells were cultured together with Tg<sup>-</sup> or Tg<sup>+</sup> BMDCs pulsed with the indicated SA lipid Ags for 48h (CTL 5–7) or for 18h (CTL6 & 51). Supernatants from the 5–7 T cell culture were assayed for IFN- $\gamma$  production by ELISA, while IFN- $\gamma$  and TNF- $\alpha$  ELISPOT was performed for T cell lines 6 and 51. (C) Cytokine producing capacity of 3 group 1 CD1-restricted T cell lines in response to PMA-Ionomycin stimulation. (D) Cytokine production from group 1 CD1-restricted T cell lines in response to SA lipid stimulation. (E) Table showing characteristics of 3 group 1

CD1-restricted SA lipid-specific T cell lines. Data representative of 2–3 independent experiments with  $n = 2$  wells/condition. \* $p < 0.05$ , \*\* $p < 0.01$ , \*\*\* $p < 0.005$  using 2-way ANOVA with Tukey's posttest.

<https://doi.org/10.1371/journal.ppat.1008443.g005>

### SA associates with group 1 CD1-expressing APCs in vivo and early endosomes subcellularly in vitro

Protective efficacy in vivo led us to question how group 1 CD1-restricted T cells could help to kill SA in vitro. To investigate this issue, we first determined which group 1 CD1-expressing antigen-presenting cells associated with SA in vivo. hCD1Tg mice were infected with USA300 SA-GFP i.v. Mice were sacrificed at 10 days post-infection and kidney lymphocytes and kidney-draining lymph nodes were isolated and processed to determine SA co-localization with APCs. Though SA-GFP mainly associated with neutrophils (here gated on  $CD11b^+Ly-6G^{hi}$  cells), these cells did not express high levels of CD1b or CD1c (Fig 7A and 7B). Rather, DCs and macrophages (gated here as  $CD11b^{hi}CD11c^{hi}$  or  $CD11b^{hi}F4/80^+$ , respectively) comprised the majority of CD1b- and CD1c-expressing cells associated with SA-GFP (Fig 7B). We further determined the subcellular localization of SA through immunofluorescence confocal microscopy. Tg<sup>+</sup> BMDCs were infected with SA and stained with antibodies against LAMP-1 (lysosomal marker), EEA-1 (marker for early endosomes), and SA. SA co-localized with LAMP-1

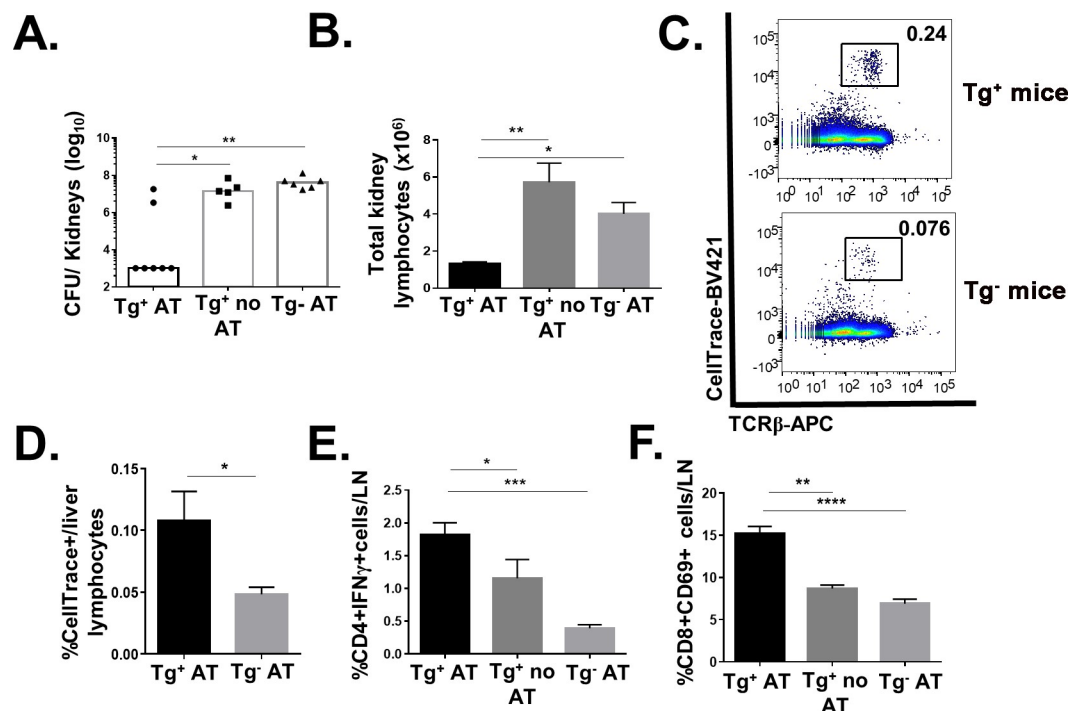


**Fig 6. Adoptive transfer of SA lipid-specific CD1b-restricted T cells protect against SA infection in hCD1Tg mice.** (A) PBS or  $2 \times 10^6$  cells of T cell line 51 labeled with CellTrace were adoptively transferred via tail vein into hCD1Tg or Tg<sup>+</sup> mice 24h prior to infection. Mice were then infected with  $2.5 \times 10^6$  CFU of SA also via tail vein and euthanized at 4 days post-infection. Kidneys were isolated for CFU enumeration. (B) Total number of kidney lymphocytes isolated from each of the 3 treatment groups. (C) Representative dot plot showing T cell line 51 is present in higher numbers as TCR $\beta^+$ CellTrace<sup>+</sup> cells in livers of infected Tg<sup>+</sup> mice compared to Tg<sup>-</sup> mice. (D) Bar graph depicts percentage of adoptively transferred T cell line 51 (TCR $\beta^+$ CellTrace<sup>+</sup>) in the liver of Tg<sup>+</sup> and Tg<sup>-</sup> recipient mice. (E) Peripheral lymph node lymphocytes stimulated with PMA-Ionomycin for 6 hours. Intracellular cytokine staining detected IFN- $\gamma$  production from CD4<sup>+</sup> lymphocytes. (F) CD69 expression on CD8<sup>+</sup> T cells in peripheral lymph nodes of infected mice. Data representative of 2 independent experiments with  $n = 3-5$  mice per group. \* $p < 0.05$ ; \*\* $p < 0.01$ ; \*\*\* $p < 0.001$ ; \*\*\*\* $p < 0.0001$ .

<https://doi.org/10.1371/journal.ppat.1008443.g006>



Infection proceeded for 18h. Data representative of 3 independent experiments with all conditions plated in triplicate. (F) BMDCs were infected as above and T cell line 51 cells were added in the presence and absence of antibodies against IFN- $\gamma$  and TNF- $\alpha$  or Granzyme B as shown. Data representative of 1 independent experiment with all conditions plated in 4x. \* $p < 0.05$ , \*\* $p < 0.01$  using 1-way ANOVA with Bonferroni's posttest or Student's t test.

<https://doi.org/10.1371/journal.ppat.1008443.g007>

and EEA-1 in areas close to the cell membrane (Fig 7C), consistent with published reports that SA can survive intracellularly in membrane-associated vacuoles of human monocyte-derived macrophages [47] and is not affected by endolysosomal acidification [48]. Loading of lipid antigens onto CD1b molecules also occurs in endolysosomal compartments [49], allowing for CD1b interaction with SA lipids after internalization of SA by the cell. Uninfected BMDCs did not show EEA1-LAMP1 colocalization (S10 Fig).

### Group 1 CD1-restricted T cells can help control of SA growth in vitro

As SA primarily associated with group 1 CD1-expressing DCs and macrophages in vivo, we used these two cell types as APCs for in vitro SA infection. Tg<sup>-</sup> and Tg<sup>+</sup>MHC-II<sup>-/-</sup> BMDCs and BMMs were infected with SA in vitro. APCs lacking MHC-II were used in order to eliminate potential complications generated from superantigen and MHC-II-mediated T cell activation, and gentamicin was added 30 minutes post-infection to kill extracellular bacteria. Despite similar infection efficiencies at time 0, at 18h post-infection only the co-culture comprised of infected Tg<sup>+</sup> BMDC and T cell line 5–7 was able to efficiently control SA replication by 10<sup>4</sup>-fold (Fig 7D, right). This demonstrated that direct Ag presentation by Tg<sup>+</sup> BMDC to cell line 5–7 was required to limit SA replication in vitro. In contrast, cross-presentation of SA lipids from infected Tg<sup>-</sup> macrophages incubated with Tg<sup>+</sup> BMDCs to cell line 5–7 was unable to control SA replication (Fig 7D, left, hatched bar). Similarly, cell line 51 was able to control SA replication through direct Tg<sup>+</sup>DC-T cell contact, though to a lesser extent than cell line 5–7 (Fig 7E). Finally, antibody blockade of IFN- $\gamma$  and TNF- $\alpha$  together or Granzyme B alone was able to reverse the protection conferred by T cell line 51 during in vitro SA infection (Fig 7F). Blocking IFN- $\gamma$  or TNF- $\alpha$  individually did not affect the ability of group 1 CD1-restricted T cells to control SA replication in culture (S11 Fig), suggesting some redundancy of these cytokines in vitro. This demonstrates the mechanism by which group 1 CD1-restricted T cells may confer protection during SA infection.

### Discussion

The findings herein are the first to demonstrate that group 1 CD1-restricted T cells are activated by SA lipids during in vitro and in vivo MRSA infection. The absence of group 2 CD1-restricted NKT cells did not affect the magnitude or kinetics of the group 1 response to systemic SA infection. Activation of the group 1 CD1-restricted T cell response was protective against SA-induced kidney pathology, and adoptive transfer of SA lipid-specific group 1 CD1-restricted T cells into infected hCD1Tg mice significantly decreased kidney SA burdens. We additionally identified multiple SA lipid species recognized by group 1 CD1-restricted T cells during systemic SA infection. Together, our study sheds light on a non-conventional lipid-reactive T cell subset that contributes to control of MRSA infection and may aid in future vaccine design to combat MRSA.

Naïve hCD1Tg mice immunized with SA lipid-pulsed BMDCs showed robust group 1 CD1-restricted T cell responses in both lymph nodes and spleen (Fig 1). Moving forward from this proof of principle experiment, primary systemic infection with SA similarly activated group 1 CD1-restricted T cells in the lymph nodes. Intriguingly, negating the effects of superantigens in SA by infecting hCD1Tg MHC-II<sup>-/-</sup> mice did not affect the magnitude of the group

1 CD1-restricted SA lipid-specific response compared with hCD1Tg WT mice, suggesting that CD4<sup>+</sup> conventional T cells do not significantly contribute to background IFN- $\gamma$  or IL-17 secretion when exposed to SA lipids in vivo (Fig 2B). We also addressed whether group 2 CD1-restricted T cells, or NKT cells, affected the magnitude of the group 1 CD1-restricted T cell response to SA lipids because NKT cells can also respond to a variety of microbial lipids including phosphatidyl glycerols and galactosyl diacylglycerols from different bacterial species [27, 50]. However, we found that the group 1 CD1-restricted T cell response to SA lipid was unaffected by the absence of NKT cells (Fig 2C). This is possibly because NKT cells are pre-activated innate-like lymphocytes that function early during bacterial infection [51], whereas the 10 day peak of the group 1 CD1-restricted T cell response more resembles that of conventional T cells during primary SA infection (Fig 3A, S3 Fig).

Interestingly, hCD1Tg mice showed markedly decreased kidney inflammation and pathology compared with Tg<sup>WT</sup> littermate control mice (Fig 3D), despite no significant differences in CFU (Fig 3C). Immunofluorescence staining showed that SA and neutrophilic infiltrates were generally contained to small circular areas in hCD1Tg kidneys, whereas large, disordered areas of neutrophils and SA were deposited in Tg<sup>WT</sup> kidneys (Fig 3E and S4 Fig). Previous studies have demonstrated that IFN- $\gamma$ /IL-17<sup>-/-</sup> mice develop spontaneous oral abscesses attributable to MRSA infection by 6–10 weeks of age due to dysregulated neutrophil and macrophage function [52]. SA-infected IFN- $\gamma$ /IL-17<sup>-/-</sup> mice also displayed neutrophilic abscesses without defined borders at 3 days post-infection compared with WT mice that had clearly defined abscesses [53]. Thus, it is possible that group 1 CD1-restricted T cell production of IFN- $\gamma$  and IL-17 in the lymph nodes in response to SA lipid can organize abscess formation downstream in the kidneys by affecting neutrophil recruitment and deposition.

Unbiased lipid fractionation and screening revealed that cardiolipins and polar phospholipids, specifically phosphatidyl glycerol (PG) species, are immunodominant SA lipids in the polyclonal infection setting (Fig 4B). SA lipid species, unlike the extensively characterized, relatively complex group 1 CD1 Mtb lipid antigens [54], are somewhat similar to mammalian lipids [41, 45]. However, lysyl-PG is one SA lipid component that is unique to bacteria and enriched in the immunodominant fraction 8 [55]. We initially hypothesized that lysyl-PG was responsible for the majority of IL-17 and IFN- $\gamma$  secretion from group 1 CD1-restricted T cells. In addition to being a uniquely bacterial lipid, lysyl-PG also enables antibiotic resistance and immune evasion [56, 57], thus leading us to speculate that group 1 CD1-restricted T cells might aid in counteracting this mechanism in SA. Contrary to this hypothesis, when lipid antigens from the lysyl-PG-deficient *fntC::erm* strain of SA were used, Fr8 retained the ability to activate group 1 CD1-restricted T cells (Fig 4D), implicating PG and not lysyl-PG species as immunodominant SA lipids. PG is known to be a CD1b-restricted T cell antigen; one previous study identified an autoreactive CD1b-restricted T cell clone from healthy human donors not known to be SA-infected that could cross-react with PG isolated from *S. aureus* and synthetic mammalian 18:0/18:1 PG [39]. This appears to differ from our results in the polyclonal setting in that hCD1Tg mice infected with SA displayed robust IL-17 secretion from group 1 CD1-restricted T cells in response to PG-rich Fr8 from SA but not to synthetic mammalian 18:0 PG (S6 Fig). Thus we hypothesize that a subset of SA PG-specific, non-autoreactive group 1 CD1-restricted T cells are induced during SA infection. SA-derived cardiolipins also activated group 1 CD1-restricted T cells in the polyclonal SA infection setting (Fig 4A). Though much larger than phosphatidyl glycerol moieties also presented by CD1b molecules [39], we suspect that CD1b has a large enough binding groove to accommodate cardiolipin species. Indeed, CD1b presents Mtb lipids with acyl chain lengths that are 80 carbons long [36]; thus we anticipate CD1b would also be able to bind and present cardiolipin. Intriguingly, the cardiolipin-enriched Fr3 selectively induced IL-17 but not IFN- $\gamma$  production from group 1 CD1-restricted

T cells (Fig 4B). This may be attributable to the binding affinity of cardiolipin-CD1 engagement with the group 1 CD1-restricted TCR, as has been shown in CD4<sup>+</sup> conventional T cells to promote T<sub>h</sub>17 differentiation [58]. It is also possible that the group 1 CD1-independent IFN- $\gamma$  production observed in Fr3-stimulated lymphocytes was mediated through TCR-independent, cytokine-driven mechanisms. The studies contained herein are the first to our knowledge to identify SA-derived cardiolipins as group 1 CD1-binding lipid antigens, though further study using cell-free target systems is needed to verify TCR dependence in these responses.

SA and gram-positive bacteria in general contain a diversity of PG species that elute differently according to the solvent gradient. It is interesting to note that not all PG-rich fractions of SA lipids induced group 1 CD1-dependent T cell secretion of cytokine (Fig 4B). A comprehensive LC-Q-TOF-MS analysis of SA lipids demonstrated that PG species of different chain lengths eluted at different times in HPLC [41], and a recent study on *Enterococcus faecalis* lipids showed similar findings [59]. Indeed, silica column fractionation of total SA lipids resulted in multiple fractions enriched with different PG species depending on the ratio of CHCl<sub>3</sub>:MeOH used (Fig 4A). It is possible that though PG species in SA contain the same polar headgroups, the differences in fatty acyl chain lengths between PG moieties may affect binding affinity to the group 1 CD1 antigenic groove and subsequent TCR engagement strength. Previous studies have shown that CD1b binds diverse sulfolipids from Mtb with the same polar headgroup but differing acyl chain lengths, which results in altered TCR recognition and T cell activation [38]. A similar mechanism could be at play regarding PG moieties from SA. Additionally, it is known that variations in the branching patterns of alkyl chains can also affect lipid Ag binding onto CD1c and downstream T cell activation [60]. Indeed, SA contains an abundance of anteiso- and iso-branched fatty acyl chains associated with PG species in the bacterial cytoplasmic membrane [61] that are not present in mammals, which may uniquely activate group 1 CD1-restricted T cells. Further characterization by GC-MS or ESI-tandem mass spectrometry is needed to determine if these subtle structural differences exist between SA PG species, and whether they contribute to immunodominance hierarchies in the polyclonal infectious setting.

Recent studies have shown that T cell production of IL-17 and IFN- $\gamma$  is essential for protection against SA in both mice and humans [16, 18, 19, 53]. Despite this, vaccine trials focused on activating CD4<sup>+</sup> conventional T cell responses specifically have largely failed in humans [13, 62]. It is therefore important to examine whether activation of non-conventional T cells during SA infection can be protective. Adoptive transfer of the group 1 CD1-restricted SA lipid-specific T cell line CTL51 decreased SA kidney burdens by  $\sim 10^4$  fold at 4 days post-infection in hCD1Tg but not Tg<sup>-/-</sup> WT mice (Fig 6A). This effect was correlated with trans-activation of CD4 and CD8 T cells in the draining lymph nodes (Fig 6E and 6F), consistent with where the group 1 CD1-restricted T cell response occurred during primary SA infection (Fig 2). The magnitude of protection afforded by the adoptively transferred SA-lipid-specific group 1 CD1-restricted T cells suggests that it will be important to elucidate how best to activate group 1 CD1-restricted T cell responses during infection, as this could provide a robust, novel protective mechanism against systemic SA infection.

Though primarily considered an extracellular pathogen, studies have shown that SA can enter into macrophages, DCs, neutrophils, and even non-phagocytic cells [63]. Our data show that SA is primarily associated with neutrophils and macrophages, and to a lesser extent with DCs in the kidney (Fig 7A and 7B). While CD1b and CD1c are highly expressed on a subset of myeloid-derived dendritic cells, neutrophils and macrophages do not express CD1b and neutrophils express only low levels of CD1c. This provided the justification for the use of macrophages and DCs for in vitro infection experiments. The co-culture of group 1 CD1-restricted

T cells with SA-infected hCD1Tg<sup>-</sup> and Tg<sup>+</sup> APCs demonstrated a critical role for direct SA lipid presentation by group 1 CD1-expressing DCs to group 1 CD1-restricted T cells in controlling SA growth (Fig 7D). Indeed, no control of SA infection was observed when infected BMM were co-incubated with SA lipid-specific T cells with uninfected Tg<sup>+</sup> BMDC help, suggesting that cross-presentation of SA lipids to Tg<sup>+</sup> DCs is not effective in halting SA replication. In contrast, control of SA in culture was orders of magnitude higher when infected Tg<sup>+</sup> DCs directly presented lipids to T cell line 5–7 (Fig 7D, bottom panel). One possible explanation for this is that BMM differentiated in culture do not express CD1b [33], and our group 1 CD1-restricted T cell lines are generally CD1b-restricted (Fig 5E). Though cell line 5–7 is both CD1b and CD1c-restricted (Fig 5E), the binding affinity of CD1b loaded with SA lipid to the cell line 5–7 TCR may be higher than the CD1c-TCR binding affinity, allowing for differential cytokine producing capacities during in vitro SA infection. This is still purely speculative, as one limitation of our study was that we could only indirectly show TCR dependence for activation in our group 1 CD1-restricted cell lines (S9 Fig). Another possibility is that SA internalized by BMM can easily escape mature phagolysosomes and kill the cells [48], which would limit TCR engagement. Dendritic cell cross presentation of SA lipids from infected macrophages may also be less efficient at activating group 1 CD1-restricted T cells because the time spent internalizing apoptotic macrophages and processing/presenting SA lipids may take too long, allowing bacteria to overgrow in the culture. Additionally, BMDCs may be more resistant to killing by SA, as one study examining DC-S. aureus interactions in vitro showed efficient control of infection of BMDCs out to 18h post-infection [64]. This would allow more time for group 1 CD1-restricted T cell activation in culture.

Finally, blockade of either TNF- $\alpha$  and IFN- $\gamma$  together or granzyme B alone was sufficient to limit the protective efficacy of group 1 CD1-restricted T cell line 51 (Fig 7F). T cell secretion of granzyme B protects against bacterial growth in a variety of infection models. Enhanced clearance of pulmonary MRSA was observed in mice with elevated granzyme B levels, a phenotype which was replicated in human neutrophil culture [65]. Though this phenotype depended on neutrophil secretion of granzyme B, it is likely that T cell production of granzyme B has similar effects. Granzyme B production from a CD4<sup>+</sup> human T cell clone also protected against Mtb growth in macrophages in vitro [66], and resistance to Mtb infection in humans is correlated with elevated MAIT cell production of granzyme B [67]. Similarly, intracellular growth of *Listeria monocytogenes* (LM) within HeLa cells and monocyte-derived dendritic cells was inhibited by human LM-specific CTL in a granzyme B-dependent manner [68], suggesting that granzyme B is broadly effective in killing multiple species of intracellular bacteria. Similarly, studies have shown that both IFN- $\gamma$  and TNF- $\alpha$  contribute to host resistance against systemic SA infection [69], and that  $\gamma\delta$  T cell production of both cytokines controlled SA replication in a mouse skin infection model [70]. Though blocking either IFN- $\gamma$  or TNF- $\alpha$  individually in vitro did not affect SA replication compared to the Tg<sup>+</sup> DC-T cell condition (S11 Fig), blocking both simultaneously enhanced replication (Fig 7F). This suggests that IFN- $\gamma$  and TNF- $\alpha$  production by group 1 CD1-restricted T cells in vitro play a redundant role in controlling SA replication.

*Staphylococcus aureus* has proven to be a stubborn pathogen to eradicate or develop vaccines against. This highlights the importance of elucidating novel pathways of T cell activation during SA infection to expand the parameters of vaccine design. The studies herein are the first to our knowledge to demonstrate that lipid-specific group 1 CD1-restricted T cells can be activated during systemic SA infection. Notably, these T cells primarily respond to SA-derived phospholipids and can control bacterial growth both in vitro and in vivo settings. These data suggest that incorporating SA lipid antigens into a multi-component subunit vaccine which

targets both unconventional and conventional T cells may be effective in helping combat this complex public health crisis.

## Materials and methods

### Ethics statement

This study was carried out in strict accordance with the recommendations in the Guide for the Care and Use of Laboratory Animals of the National Institutes of Health. The protocol was approved by the Animal Care and Use Committee of the Northwestern University (Protocol number: IS00001659).

### Mouse strains

hCD1Tg mice (Line 78 and Line 64) in the B6 background were generated in our lab as previously described [32]. hCD1Tg mice were also crossed onto B6 MHC-II-deficient or CD1d-deficient background [71]. Most in vivo infection experiments used hCD1Tg (Line 78) mice expressing CD1b and CD1c but not CD1a due to better breeding performance. Proof of principle experiments used hCD1Tg (Line 64) mice expressing CD1a, CD1b and CD1c in a tissue-specific, physiologically relevant manner.

### Bacterial strains, media, and culture conditions

Mouse intravenous infections with *Staphylococcus aureus* (SA) were carried out using the methicillin resistant USA300 strain LAC or LAC-GFP [72]. SA was grown shaking overnight in TSA broth (MP Biomedicals, Solon, OH) at 37°C, 220 rpm. A marked *fmtC::erm* insertional disruption in strain LAC was generated by bacteriophage-mediated transduction using  $\phi$ 11 containing DNA from transposon mutant NE1360 of the Nebraska transposon mutant library [73]. SA lipids were isolated from either WT LAC or *fmtC::erm* LAC.

### Primary cell preparation

Single cell suspensions were prepared from livers, spleens, pooled peripheral lymph nodes, and/or kidneys of infected or immunized hCD1Tg mice. Lymphocytes were isolated from livers and kidneys using a 37.5% Percoll gradient centrifugation. At times,  $\alpha\beta$  T cells were enriched through depletion of B220<sup>+</sup>, CD11c<sup>+</sup>, F4/80<sup>+</sup>, Ly-6G<sup>+</sup>, MHC-II<sup>+</sup>, and TCR $\gamma\delta$ <sup>+</sup> T cells using biotin-conjugated antibodies (BioLegend, San Diego, CA) and the Dynabeads depletion kit (ThermoFisher Scientific, Waltham, MA). BMDCs were derived from mouse bone marrow progenitors using GM-CSF and IL-4 (PeproTech) as previously described [74]. BMM were derived from bone marrow progenitors using complete DMEM supplemented with 30% L929-conditioned medium or 20ng/mL recombinant MCSF (PeproTech).

### Antibodies and flow cytometry

CD1a-PE, CD1b-PE, CD1c-FITC, B220-PerCPCy5.5, F4/80-APC, CD11c- BV421, CD8-BV510, CD4-PerCPCy5.5, IFN- $\gamma$ -APC, IL-17-PE, Granzyme B-BV421, and TNF- $\alpha$ -FITC antibodies were purchased from BioLegend (San Diego, CA). TCR- $\beta$ -BV421, anti-V $\beta$ 3 and 4-PE, and anti-V $\beta$ 5.1/5.2-APC were obtained from BD biosciences (San Jose, CA). For flow cytometry, single cell suspensions from organs were incubated with 2.4G2 FcR blocking antibody for 10 minutes and then stained in HBSS-2% FBS containing 50  $\mu$ g/mL gentamicin. Samples were run on the FACS Canto II flow cytometer (BD Biosciences, San Jose, CA). Analysis of flow cytometry data was performed on FlowJo software (Tree Star, Inc). S12 Fig shows

the gating strategies employed for the FACS plots of group 1 CD1-restricted T cells in the polyclonal setting in Fig 3 and group 1 CD1-restricted T cell line functional assays in Fig 5.

### Lipid isolation from *Staphylococcus aureus*

USA300 SA-derived total lipid was isolated from overnight cultures of USA300 WT or *fmtC::erm* grown in TSB, shaking at 220rpm, 37°C. Bacteria were pelleted, washed in PBS, and resuspended in 50 nM KH<sub>2</sub>PO<sub>4</sub> buffer containing 2 µg/mL lysostaphin in order to lyse the peptidoglycan cell wall and release protoplasts. Bacteria pellet were washed with PBS and then resuspended in 100% EtOH for further processing. Total SA lipids were isolated from protoplasts using a CHCl<sub>3</sub>-MeOH Bligh-Dyer extraction procedure [75]. Sub-fractionation was carried out using silica gel column chromatography (0.5 x 20cm) using a stepwise elution procedure with chloroform, acetone, and methanol in chloroform as solvents (15mL per fraction). Lipids were characterized by 1D- and 2D-TLC using hexane/diethyl ether/acetic acid (85:15:1, v/v) for 1-D TLC and chloroform/methanol/28% ammonia/toluene (64:30:6:10, v/v) as solvent A and chloroform/methanol/acetone/acetic acid/water/toluene (70:30:5:4:1:10, v/v) as solvent B. Lipid visualization was performed with 10% sulfuric acid in methanol with heating or using phosphomolybdate reagent to detect phospholipids. [76]. Lipids were also characterized by electrospray ionization tandem mass spectrometry (ESI-MS/MS) using the AB Sciex 6500 QTRAP mass spectrometer.

### Intravenous SA infection and DC immunization of mice

*S. aureus* overnight cultures were diluted 1:100 and subsequently grown to mid-log phase (~3 hours) shaking at 37°C, 220 rpm. Bacteria were washed in PBS and mice were infected with 3-5x10<sup>6</sup> CFU in sterile PBS via tail vein injection. At indicated times, lymphocytes isolated from various organs were harvested and analyzed by flow cytometry and ELISPOT assays. Kidney homogenates from infected mice were plated on tryptic soy agar (TSA) plates to determine viable CFU. For immunization, hCD1Tg MHC-II<sup>-/-</sup> DCs were pulsed overnight with total SA lipids (10 µg/mL). 10<sup>6</sup> BMDCs were injected intraperitoneally into mice and spleens and lymph nodes isolated for ELISPOT assays 7 days post-immunization.

### ELISPOT assays

Multiscreen-IP plates (Millipore-Sigma) were coated with 5 µg/mL anti-IFN-γ (clone AN-18, BioLegend) or anti-IL-17 (clone eBioCK15A5, Thermo Scientific), washed, and blocked with RPMI-10. Lymphocytes from spleens or pooled peripheral lymph nodes from immunized or infected mice were added to each well containing 5x10<sup>4</sup> hCD1Tg<sup>-</sup> or Tg<sup>+</sup>MHC-II<sup>-/-</sup> BMDCs pulsed with total SA lipids or lipid fractions, purified mammalian 16:0–18:1 cardiolipin, mammalian 18:0 phosphatidyl glycerol, or bacteria-derived 16:0 lysyl PG (Avanti Polar lipids, Alabaster, AB). Plates were incubated at 37°C for 20 h and developed using an Alkaline Phosphatase Conjugate Substrate Kit according to manufacturer's instructions (Bio-Rad Laboratories, Carlsbad, CA). IFN-γ or IL-17-producing cells were quantified using an ImmunoSpot reader (Cellular Technologies, Ltd., Shaker Heights, OH).

### Generation of group 1 CD1-restricted T cell lines

Lymphocytes isolated from SA-infected hCD1Tg mice were cultured for 4 days in RPMI-10 and subsequently in supplemented Eagle's minimum essential medium with 10U/mL recombinant mouse IL-2 (PeproTech, Rocky Hill, NJ) [77]. T cell lines were re-stimulated weekly

with irradiated SA lipid pulsed hCD1Tg MHC-II<sup>-/-</sup> BMDCs. T cell clones 6, 51, and 5–7 were generated via limiting dilution cloning.

### Adoptive transfer of group 1 CD1-restricted T cell lines

T cell line 51 was labeled with CellTrace Violet (Thermo Scientific) dye prior to injection into mice.  $2 \times 10^6$  cells in 200  $\mu$ L of PBS were injected into hCD1Tg or Tg<sup>-</sup> sex-matched mice via tail vein 1 day prior to infection. Control hCD1Tg mice received PBS alone. All mice were infected with  $2 \times 10^6$  CFU of SA USA300 via tail vein at day 0 and euthanized at 4 days post-infection. Livers, spleens, peripheral lymph nodes and kidneys were isolated for CFU enumeration or functional experiments. Lymphocytes from these organs were stimulated with phorbol myristate acetate and ionomycin (PMA-Iono) at a concentration of 20 ng/mL and 1  $\mu$ M, respectively, for 6 h. Brefeldin A (10  $\mu$ g/mL) was added to the cells at 2 h post-stimulation to detect intracellular cytokine production.

### In vitro infections

BMM ( $5 \times 10^4$ /well) and BMDC ( $10^5$  cells/well) were plated in triplicate in 48 well plates and infected with SA USA300 at MOI = 0.2. After 30 min, the medium was replaced with DMEM containing 100  $\mu$ g/mL gentamicin to kill extracellular bacteria for 30 minutes. Cells were then washed twice in warm PBS and a portion of BMM and BMDC were lysed in the wells with 300  $\mu$ L sterile H<sub>2</sub>O to plate intracellular bacteria for Time 0 CFU enumeration. The remainder of the cells received either media alone or had uninfected BMDCs ( $10^5$ /well), BMMs ( $5 \times 10^4$ /well), or T cells ( $4 \times 10^5$ /well) added to the wells. Some experiments included antibody blockade of cytokine production; 1  $\mu$ g/well was added of each of the following:  $\alpha$ -IFN- $\gamma$  (clone AN-18),  $\alpha$ -TNF- $\alpha$  (clone 6B8), or  $\alpha$ -Granzyme B (clone QA16A02) (all from BioLegend). For antibody blocking experiments, all conditions were plated in groups of 4. Cells were spun down to enable contact and incubated for 18 hours at 37°C. Plates were then spun down at 2400 rpm x 15 minutes to pellet SA, supernatant removed, and cells lysed in the wells with 300  $\mu$ L sterile H<sub>2</sub>O. Samples were serially diluted and spot-plated for CFU enumeration on TSA plates containing 5  $\mu$ g/mL erythromycin.

### Immunofluorescence on APCs

BMDCs and BMMs ( $10^6$  cells) were plated onto glass coverslips coated with poly-L-lysine inside 12-well plates and allowed to adhere for 1 hour. Cells were left uninfected or were infected with SA at MOI = 5 for 45 minutes. Cells were then washed twice with PBS and resuspended in DMEM containing 100  $\mu$ g/mL gentamicin to kill extracellular bacteria for 30 minutes at 37°C. Cells were washed, fixed with 10% PBS-buffered formalin containing zinc, and stained with the following primary antibodies in PBS + 1% BSA: polyclonal rabbit anti-mouse EEA-1, rat anti-mouse LAMP1 (clone 1D4B), and mouse anti-Staphylococcus aureus (clone 704) from Abcam (Cambridge, MA). Alexa fluor-conjugated secondary antibodies were goat anti-mouse IgG H&L-AF488 (Abcam), goat anti-rat IgG H&L-AF568 and goat anti-rabbit IgG H&L-AF647 (both from ThermoFisher, Waltham, MA). Cells were incubated in Vectashield + DAPI and placed onto glass slides for imaging. Microscopy was performed using a confocal Nikon A1R (A) spectral microscope (Nikon, Melville, NY).

### Immunofluorescence on paraffin-embedded sections

Immunofluorescence on kidneys was performed as previously described [78]. Briefly, paraffin-embedded kidneys deparaffinized with xylene and rehydrated with graded ethanol washes.

Antigen retrieval was performed using sodium citrate buffer in a pressure cooker. Endogenous peroxidases were quenched with 10% H<sub>2</sub>O<sub>2</sub>. Background Buster blocking solution (Innovex Biosciences, Richmond, CA) was applied to each sample prior to incubation in primary antibody. Slides were then incubated sequentially with rabbit polyclonal anti-SA (Abcam) and rat anti-mouse Ly-6G (clone 1A8) for 1 hour at room temperature or overnight at 4°C. Slides were then incubated sequentially with goat anti-rat AF-555 (Invitrogen) or goat anti-rabbit AF488 (Abcam) for 1 hour at room temperature. Slides were then mounted using Vectashield Antifade Reagent with DAPI (Vector Labs). Slides were imaged at 25°C, 20x magnification, using the Nikon A1 HD25 confocal microscope (Nikon Instruments Inc, Melville, NY). Images were analyzed with NIS Elements Viewer 4.20 software.

### Statistical analysis

Statistical analyses were performed using Prism software (GraphPad Software, Inc., San Diego, CA). Significant differences at 95% confidence or above are depicted with asterisks on each graph.

### Supporting information

**S1 Fig. SA lipid-specific group 1 CD1-restricted T cell responses can be detected in hCD1Tg mice expressing CD1a, -b, and -c during systemic SA infection.** hCD1Tg mice expressing CD1a, -b, and -c (Tg64) were infected with 5x10<sup>6</sup> CFU of SA USA300 via tail vein. Mice were sacrificed at 10 days post-infection and peripheral lymph nodes were isolated. Lymphocytes were cultured overnight with SA lipid pulsed or unpulsed Tg<sup>-</sup> and Tg<sup>+</sup> MHC II<sup>-/-</sup> BMDCs and assayed for IL-17A production via ELISPOT. Data representative of 2 independent experiments with n = 5–7 mice per experiment. \*p<0.05 using a two-tailed Student's t test.

(TIF)

**S2 Fig. Group 1 CD1-restricted T cell responses against SA lipids cannot be detected in the kidney at 10 days post-infection.** hCD1Tg mice were infected with 5x10<sup>6</sup> CFU of USA300 via tail vein. Mice were euthanized at 10 days post-infection and lymphocytes from the kidney and associated lymph nodes were isolated and cultured with the indicated BMDC targets overnight. IFN-γ (right) and IL-17A (left) production was assessed by ELISPOT assays. Data representative of 2 independent experiments with n = 3–4 mice per experiment.

(TIF)

**S3 Fig. Activation kinetics of conventional T cells and the expression of group 1 CD1 during the course of SA infection.** (A) Tg<sup>WT</sup> mice were infected with 5x10<sup>6</sup> CFU of USA300 i.v. and sacrificed at the indicated times post-infection. Lymphocytes from lymph nodes were stained with T cell-specific antibodies for FACS. Cells were gated on either TCRβ<sup>+</sup>CD4<sup>+</sup>NK1.1<sup>-</sup> cells or TCRβ<sup>+</sup>CD8<sup>+</sup> cells and output for CD69 expression. (B, C) hCD1Tg mice were infected as above and sacrificed at the indicated times. Lymphocytes from pooled peripheral lymph nodes were analyzed by FACS for CD1b and CD1c expression at different times post-infection. Data representative of 4 independent experiments with n = 4–5 mice per time point. \*p<0.05; \*\*p<0.01; \*\*\*p<0.005 using one-way ANOVA with Tukey's post-test.

(TIF)

**S4 Fig. hCD1Tg mice display less kidney pathology than Tg<sup>-</sup> WT mice in response to SA infection.** hCD1Tg and Tg<sup>-</sup> WT littermate control mice were infected with 3x10<sup>6</sup> CFU of SA via tail vein. Mice were euthanized at 10 days post-infection and kidneys were isolated and

processed for H&E staining. Panels show whole kidney sections containing areas of inflammation and mature abscess formation, with Tg<sup>-</sup> WT mice more affected than hCD1Tg<sup>+</sup> mice. Data representative of 2 independent experiments with n = 4 mice per group.

(TIF)

**S5 Fig. SA lipid fractions enriched in phospholipids are heterogeneous.** (A) Table showing percentage of PG species present in each PG-rich fraction classified according to acyl chain length. Cardiolipin-enriched Fraction 3 has the same chain length distribution as it is simply a dimer of PG species. (B) Lipid fractions were subjected to TLC separation using chloroform:methanol:acetone:acetic acid:water:toluene (70:30:5:4:1:10, v/v) as a solvent system. Phospholipids in each fraction (right panel) were visualized using phosphomolybdate reagent (blue spots) as described in Vaskovsky *et al.* [76]. Total lipids were visualized by “charring” or heating the same blot used to visualize phospholipids (left). Increasing concentrations of lysyl-PG is the main distinguishing characteristic between PG-enriched fractions 6, 7, and 8.

(TIF)

**S6 Fig. USA300 *fmcC::erm* mutant specifically lacks lysyl-PG but retains PG species.** Mass spectra showing that the *fmcC::erm* mutant strain of SA (bottom panel) retains all other major SA lipid moieties except for lysyl-PG species.

(TIF)

**S7 Fig. Purified mammalian cardiolipin, PG and synthetic lysyl-PG cannot activate group 1 CD1-restricted T cells from SA-infected mice.** hCD1Tg mice were infected with 3x10<sup>6</sup> CFU of SA via tail vein. Mice were euthanized at 10 days post-infection and lymphocytes from pooled peripheral lymph nodes were put into IL-17A ELISPOT. Data representative of 2 independent experiments with n = 4 mice per experiment. \*p<0.05 using two-way ANOVA with Tukey's posttest.

(TIF)

**S8 Fig. SA lipids enhance BMDC activation to similar levels in Tg<sup>-</sup> and Tg<sup>+</sup> BMDCs, irrespective of group 1 CD1 expression.** (A, B) Quantification of CD86 (A), CD1b, and CD1c (B) expression in unstimulated or SA lipid stimulated Tg<sup>-</sup> and Tg<sup>+</sup> BMDCs. (C) Tg<sup>-</sup> and Tg<sup>+</sup> DCs produced similar levels of IL-6 in response to SA lipids. Tg<sup>-</sup> and Tg<sup>+</sup> BMDCs were stimulated with the indicated SA lipids/fractions for 12h and supernatants were assayed for IL-6 production by ELISA.

(TIF)

**S9 Fig. MyD88-independent cytokine production by group 1 CD1-restricted SA-lipid-specific T cell lines.** T cell lines 51, 6, and 5–7 were stimulated with Tg<sup>-</sup> and Tg<sup>+</sup> BMDCs coated with SA lipids and lacking the MyD88 adaptor protein for NFκB signaling. Cells were co-cultured overnight (T cell line 6, 51) or for 48h (T cell line 5–7) and IFN-γ ELISPOT (T cell line 6, 51) or ELISA (T cell line 5–7) was performed. Data shown is after subtracting background from Tg<sup>-</sup> or Tg<sup>+</sup> BMDC unstimulated conditions. Data representative of 2–3 independent experiments with each condition plated in duplicate. \*\*p<0.01 using two-way ANOVA with Tukey's posttest.

(TIF)

**S10 Fig. EEA1 and LAMP1 colocalization depends on SA infection in vitro.** Immunofluorescence staining against LAMP1, EEA1, and SA was conducted on uninfected or SA-infected BMDCs. Data representative of 2 independent experiments with all conditions stained in triplicate.

(TIF)

**S11 Fig. Blocking of granzyme B but not TNF- $\alpha$  or IFN- $\gamma$  individually reduce the ability of cell line 5–7 to help control SA replication in vitro.** BMDCs were infected with SA as in Fig 7 and infection proceeded for 13h. Some conditions included antibody against IFN- $\gamma$  or TNF- $\alpha$  or granzyme B in each well. Cells were lysed in the wells and bacteria pelleted and plated for CFU enumeration. All conditions were plated in triplicate. Data representative of 3 independent experiments. \* $p < 0.05$  using Student's t test.  
(TIF)

**S12 Fig. Gating strategies for Figs 3B and 5C.** Fig 3B is gated on lymphocytes from pooled peripheral lymph nodes of hCD1Tg<sup>+</sup> mice after depletion of endogenous antigen presenting cells and  $\gamma\delta$  T cells. Fig 5C is gated on lymphocytes from the primary T cell line CTL 5–7.  
(TIF)

## Acknowledgments

We thank the members of the Wang lab for helpful discussions. We also thank the Northwestern Robert H. Lurie Cancer Center Flow Cytometry Core Facility for cell sorting, Mouse Histology and Phenotyping Core Facility for help with histological sectioning and staining, and the Center for Advanced Microscopy for assisting with confocal imaging.

## Author Contributions

**Conceptualization:** Lavanya Visvabharathy, Chyung-Ru Wang.

**Data curation:** Lavanya Visvabharathy, Samantha Genardi, Liang Cao, Ying He, Francis Alonzo, III, Evgeny Berdyshev.

**Formal analysis:** Lavanya Visvabharathy, Chyung-Ru Wang.

**Funding acquisition:** Chyung-Ru Wang.

**Investigation:** Lavanya Visvabharathy, Samantha Genardi, Liang Cao, Ying He, Francis Alonzo, III, Evgeny Berdyshev.

**Supervision:** Chyung-Ru Wang.

**Writing – original draft:** Lavanya Visvabharathy, Chyung-Ru Wang.

**Writing – review & editing:** Samantha Genardi, Liang Cao, Francis Alonzo, III, Evgeny Berdyshev.

## References

1. Hidron AI, Edwards JR, Patel J, Horan TC, Sievert DM, Pollock DA, et al. NHSN annual update: antimicrobial-resistant pathogens associated with healthcare-associated infections: annual summary of data reported to the National Healthcare Safety Network at the Centers for Disease Control and Prevention, 2006–2007. *Infection control and hospital epidemiology: the official journal of the Society of Hospital Epidemiologists of America*. 2008; 29(11):996–1011. Epub 2008/10/25. <https://doi.org/10.1086/591861> PMID: 18947320.
2. Lowy FD. Staphylococcus aureus infections. *The New England journal of medicine*. 1998; 339(8):520–32. <https://doi.org/10.1056/NEJM199808203390806> PMID: 9709046.
3. Casey JA, Cosgrove SE, Stewart WF, Pollak J, Schwartz BS. A population-based study of the epidemiology and clinical features of methicillin-resistant Staphylococcus aureus infection in Pennsylvania, 2001–2010. *Epidemiology and infection*. 2012; 1–14. Epub 2012/08/30. <https://doi.org/10.1017/S0950268812001872> PMID: 22929058.
4. Datta P, Chander J. Characterization of methicillin-resistant Staphylococcus aureus isolated from skin and soft tissue infections in relation to staphylococcal cassette chromosome type. *International journal*

- of infectious diseases: IJID: official publication of the International Society for Infectious Diseases. 2013; 17(11):e1085. <https://doi.org/10.1016/j.ijid.2013.04.014> PMID: 23777596.
5. Datta R, Shah A, Huang SS, Cui E, Nguyen V, Welbourne SJ, et al. High nasal burden of methicillin-resistant *Staphylococcus aureus* increases risk of invasive disease. *Journal of clinical microbiology*. 2014; 52(1):312–4. <https://doi.org/10.1128/JCM.01606-13> PMID: 24153126; PubMed Central PMCID: PMC3911445.
  6. David MZ, Daum RS, Bayer AS, Chambers HF, Fowler VG Jr., Miller LG, et al. *Staphylococcus aureus* bacteremia at 5 US academic medical centers, 2008–2011: significant geographic variation in community-onset infections. *Clinical infectious diseases: an official publication of the Infectious Diseases Society of America*. 2014; 59(6):798–807. <https://doi.org/10.1093/cid/ciu410> PMID: 24879783; PubMed Central PMCID: PMC4200044.
  7. Lee WS, Chen YC, Chen HP, Chen TH, Cheng CY. Vertebral osteomyelitis caused by vancomycin-tolerant methicillin-resistant *Staphylococcus aureus* bacteremia: Experience with teicoplanin plus fosfomicin combination therapy. *Journal of microbiology, immunology, and infection = Wei mian yu gan ran za zhi*. 2013. Epub 2013/11/26. <https://doi.org/10.1016/j.jmii.2013.09.002> PMID: 24269007.
  8. Goto M, Schweizer ML, Vaughan-Sarrazin MS, Perencevich EN, Livorsi DJ, Diekema DJ, et al. Association of Evidence-Based Care Processes With Mortality in *Staphylococcus aureus* Bacteremia at Veterans Health Administration Hospitals, 2003–2014. *JAMA Intern Med*. 2017; 177(10):1489–97. <https://doi.org/10.1001/jamainternmed.2017.3958> PMID: 28873140; PubMed Central PMCID: PMC5710211.
  9. Nelson RE, Jones M, Liu CF, Samore MH, Evans ME, Graves N, et al. The impact of healthcare-associated methicillin-resistant *Staphylococcus aureus* infections on post-discharge healthcare costs and utilization. *Infection control and hospital epidemiology: the official journal of the Society of Hospital Epidemiologists of America*. 2015; 36(5):534–42. <https://doi.org/10.1017/ice.2015.22> PMID: 25715806.
  10. Kourtis AP, Hatfield K, Baggs J, Mu Y, See I, Epton E, et al. Vital Signs: Epidemiology and Recent Trends in Methicillin-Resistant and in Methicillin-Susceptible *Staphylococcus aureus* Bloodstream Infections—United States. *MMWR Morb Mortal Wkly Rep*. 2019; 68(9):214–9. <https://doi.org/10.15585/mmwr.mm6809e1> PMID: 30845118; PubMed Central PMCID: PMC6421967 potential conflicts of interest. No potential conflicts of interest were disclosed.
  11. Jansen KU, Girgenti DQ, Scully IL, Anderson AS. Vaccine review: "Staphylococcus aureus vaccines: problems and prospects". *Vaccine*. 2013; 31(25):2723–30. <https://doi.org/10.1016/j.vaccine.2013.04.002> PMID: 23624095.
  12. Proctor RA. Challenges for a universal *Staphylococcus aureus* vaccine. *Clinical infectious diseases: an official publication of the Infectious Diseases Society of America*. 2012; 54(8):1179–86. <https://doi.org/10.1093/cid/cis033> PMID: 22354924.
  13. Giersing BK, Dastgheyb SS, Modjarrad K, Moorthy V. Status of vaccine research and development of vaccines for *Staphylococcus aureus*. *Vaccine*. 2016; 34(26):2962–6. <https://doi.org/10.1016/j.vaccine.2016.03.110> PMID: 27105559.
  14. Bobrovnik SA, Liashchenko KP. [Immune response and the formation of immunologic memory to *Staphylococcus* in mice of different genotypes]. *Zhurnal mikrobiologii, epidemiologii, i immunobiologii*. 1985;(6):64–8. PMID: 4041103.
  15. Ekstedt RD. Immune response to surface antigens of *Staphylococcus aureus* and their role in resistance to staphylococcal disease. *Annals of the New York Academy of Sciences*. 1974; 236(0):203–20. <https://doi.org/10.1111/j.1749-6632.1974.tb41492.x> PMID: 4214129.
  16. Joshi A, Pancari G, Cope L, Bowman EP, Cua D, Proctor RA, et al. Immunization with *Staphylococcus aureus* iron regulated surface determinant B (IsdB) confers protection via Th17/IL17 pathway in a murine sepsis model. *Human vaccines & immunotherapeutics*. 2012; 8(3):336–46. <https://doi.org/10.4161/hv.18946> PMID: 22327491; PubMed Central PMCID: PMC3426080.
  17. Yu W, Wang L, Wang M, Liu S, Li W, Wang X, et al. Identification and characterization of CD4(+) T cell epitopes on manganese transport protein C of *Staphylococcus aureus*. *Microb Pathog*. 2017; 112:30–7. <https://doi.org/10.1016/j.micpath.2017.09.045> PMID: 28942173.
  18. Kolata JB, Kuhbandner I, Link C, Normann N, Vu CH, Steil L, et al. The Fall of a Dogma? Unexpected High T-Cell Memory Response to *Staphylococcus aureus* in Humans. *The Journal of infectious diseases*. 2015. <https://doi.org/10.1093/infdis/jiv128> PMID: 25737563.
  19. Murphy AG, O’Keeffe KM, Lalor SJ, Maher BM, Mills KH, McLoughlin RM. *Staphylococcus aureus* infection of mice expands a population of memory gamma delta T cells that are protective against subsequent infection. *Journal of immunology*. 2014; 192(8):3697–708. <https://doi.org/10.4049/jimmunol.1303420> PMID: 24623128; PubMed Central PMCID: PMC3979672.
  20. Ma CS, Chew GY, Simpson N, Priyadarshi A, Wong M, Grimbacher B, et al. Deficiency of Th17 cells in hyper IgE syndrome due to mutations in STAT3. *The Journal of experimental medicine*. 2008; 205

- (7):1551–7. <https://doi.org/10.1084/jem.20080218> PMID: 18591410; PubMed Central PMCID: PMC2442632.
21. Utay NS, Roque A, Timmer JK, Morcock DR, DeLeage C, Somasunderam A, et al. MRSA Infections in HIV-Infected People Are Associated with Decreased MRSA-Specific Th1 Immunity. *PLoS Pathog*. 2016; 12(4):e1005580. <https://doi.org/10.1371/journal.ppat.1005580> PMID: 27093273; PubMed Central PMCID: PMC4836670.
  22. Marchitto MC, Dillen CA, Liu H, Miller RJ, Archer NK, Ortines RV, et al. Clonal Vgamma6(+)Vdelta4(+) T cells promote IL-17-mediated immunity against *Staphylococcus aureus* skin infection. *Proceedings of the National Academy of Sciences of the United States of America*. 2019; 116(22):10917–26. <https://doi.org/10.1073/pnas.1818256116> PMID: 31088972; PubMed Central PMCID: PMC6561199.
  23. Van Rhijn I, Ly D, Moody DB. CD1a, CD1b, and CD1c in immunity against mycobacteria. *Adv Exp Med Biol*. 2013; 783:181–97. [https://doi.org/10.1007/978-1-4614-6111-1\\_10](https://doi.org/10.1007/978-1-4614-6111-1_10) PMID: 23468110.
  24. Brigl M, Brenner MB. CD1: antigen presentation and T cell function. *Annual review of immunology*. 2004; 22:817–90. <https://doi.org/10.1146/annurev.immunol.22.012703.104608> PMID: 15032598.
  25. Siddiqui S, Visvabharathy L, Wang C-R. Role of Group 1 CD1-restricted T Cells in Infectious Disease. *Frontiers in immunology*. 2015; 6. <https://doi.org/10.3389/fimmu.2015.00337> PMID: 26175733
  26. Doisne JM, Soulard V, Becourt C, Amniai L, Henrot P, Havenar-Daughton C, et al. Cutting edge: crucial role of IL-1 and IL-23 in the innate IL-17 response of peripheral lymph node NK1.1-invariant NKT cells to bacteria. *J Immunol*. 2011; 186(2):662–6. Epub 2010/12/21. <https://doi.org/10.4049/jimmunol.1002725> PMID: 21169541.
  27. Tatituri RV, Watts GF, Bhowruth V, Barton N, Rothchild A, Hsu FF, et al. Recognition of microbial and mammalian phospholipid antigens by NKT cells with diverse TCRs. *Proceedings of the National Academy of Sciences of the United States of America*. 2013; 110(5):1827–32. <https://doi.org/10.1073/pnas.1220601110> PMID: 23307809; PubMed Central PMCID: PMC3562825.
  28. Trottein F, Paget C. Natural Killer T Cells and Mucosal-Associated Invariant T Cells in Lung Infections. *Frontiers in immunology*. 2018; 9:1750. <https://doi.org/10.3389/fimmu.2018.01750> PMID: 30116242; PubMed Central PMCID: PMC6082944.
  29. Chandra S, Kronenberg M. Activation and Function of iNKT and MAIT Cells. *Advances in immunology*. 2015; 127:145–201. <https://doi.org/10.1016/bs.ai.2015.03.003> PMID: 26073984.
  30. Brigl M, Bry L, Kent SC, Gumperz JE, Brenner MB. Mechanism of CD1d-restricted natural killer T cell activation during microbial infection. *Nature immunology*. 2003; 4(12):1230–7. <https://doi.org/10.1038/ni1002> PMID: 14578883.
  31. Kwiecinski J, Rhost S, Lofbom L, Blomqvist M, Mansson JE, Cardell SL, et al. Sulfatide attenuates experimental *Staphylococcus aureus* sepsis through a CD1d-dependent pathway. *Infection and immunity*. 2013; 81(4):1114–20. <https://doi.org/10.1128/IAI.01334-12> PMID: 23340309; PubMed Central PMCID: PMC3639588.
  32. Felio K, Nguyen H, Dascher CC, Choi HJ, Li S, Zimmer MI, et al. CD1-restricted adaptive immune responses to Mycobacteria in human group 1 CD1 transgenic mice. *The Journal of experimental medicine*. 2009; 206(11):2497–509. <https://doi.org/10.1084/jem.20090898> PMID: 19808251; PubMed Central PMCID: PMC2768849.
  33. Zhao J, Siddiqui S, Shang S, Bian Y, Bagchi S, He Y, et al. Mycolic acid-specific T cells protect against *Mycobacterium tuberculosis* infection in a humanized transgenic mouse model. *Elife*. 2015; 4. <https://doi.org/10.7554/eLife.08525> PMID: 26652001; PubMed Central PMCID: PMC4718816.
  34. Montamat-Sicotte DJ, Millington KA, Willcox CR, Hingley-Wilson S, Hackforth S, Innes J, et al. A mycolic acid-specific CD1-restricted T cell population contributes to acute and memory immune responses in human tuberculosis infection. *The Journal of clinical investigation*. 2011; 121(6):2493–503. <https://doi.org/10.1172/JCI46216> PMID: 21576820; PubMed Central PMCID: PMC3104771.
  35. Ulrichs T, Moody DB, Grant E, Kaufmann SH, Porcelli SA. T-cell responses to CD1-presented lipid antigens in humans with *Mycobacterium tuberculosis* infection. *Infection and immunity*. 2003; 71(6):3076–87. <https://doi.org/10.1128/IAI.71.6.3076-3087.2003> PMID: 12761085; PubMed Central PMCID: PMC155760.
  36. Rhijn IV, Iwany SK, Fodran P, Cheng TY, Gapin L, Minnaard AJ, et al. CD1b-mycolic acid tetramers demonstrate T-cell fine specificity for mycobacterial lipid tails. *Eur J Immunol*. 2017. <https://doi.org/10.1002/eji.201747062> PMID: 28665555.
  37. de Jong A, Cheng TY, Huang S, Gras S, Birkinshaw RW, Kasmar AG, et al. CD1a-autoreactive T cells recognize natural skin oils that function as headless antigens. *Nature immunology*. 2014; 15(2):177–85. <https://doi.org/10.1038/ni.2790> PMID: 24362891; PubMed Central PMCID: PMC3932764.
  38. Garcia-Alles LF, Collmann A, Versluis C, Lindner B, Guiard J, Maveyraud L, et al. Structural reorganization of the antigen-binding groove of human CD1b for presentation of mycobacterial sulfoglycolipids. *Proceedings of the National Academy of Sciences of the United States of America*. 2011; 108

- (43):17755–60. <https://doi.org/10.1073/pnas.1110118108> PMID: 22006319; PubMed Central PMCID: PMC3203780.
39. Van Rhijn I, van Berlo T, Hilmenyuk T, Cheng TY, Wolf BJ, Tatituri RV, et al. Human autoreactive T cells recognize CD1b and phospholipids. *Proceedings of the National Academy of Sciences of the United States of America*. 2016; 113(2):380–5. <https://doi.org/10.1073/pnas.1520947112> PMID: 26621732; PubMed Central PMCID: PMC4720340.
  40. Reinink P, Souter MNT, Cheng TY, van Gorkom T, Lenz S, Kubler-Kielb J, et al. CD1b presents self and *Borrelia burgdorferi* diacylglycerols to human T cells. *European journal of immunology*. 2019. <https://doi.org/10.1002/eji.201847949> PMID: 30854633.
  41. Hewelt-Belka W, Nakonieczna J, Belka M, Baczek T, Namiesnik J, Kot-Wasik A. Comprehensive methodology for *Staphylococcus aureus* lipidomics by liquid chromatography and quadrupole time-of-flight mass spectrometry. *J Chromatogr A*. 2014; 1362:62–74. <https://doi.org/10.1016/j.chroma.2014.08.020> PMID: 25160958.
  42. Li M, Diep BA, Villaruz AE, Braughton KR, Jiang X, DeLeo FR, et al. Evolution of virulence in epidemic community-associated methicillin-resistant *Staphylococcus aureus*. *Proceedings of the National Academy of Sciences of the United States of America*. 2009; 106(14):5883–8. Epub 2009/03/19. <https://doi.org/10.1073/pnas.0900743106> PMID: 19293374; PubMed Central PMCID: PMC2667066.
  43. Tebartz C, Horst SA, Sparwasser T, Huehn J, Beineke A, Peters G, et al. A major role for myeloid-derived suppressor cells and a minor role for regulatory T cells in immunosuppression during *Staphylococcus aureus* infection. *J Immunol*. 2015; 194(3):1100–11. <https://doi.org/10.4049/jimmunol.1400196> PMID: 25548227.
  44. Cheng AG, Kim HK, Burts ML, Krausz T, Schneewind O, Missiakas DM. Genetic requirements for *Staphylococcus aureus* abscess formation and persistence in host tissues. *FASEB J*. 2009; 23(10):3393–404. <https://doi.org/10.1096/fj.09-135467> PMID: 19525403; PubMed Central PMCID: PMC2747682.
  45. Kuhn S, Slavetinsky CJ, Peschel A. Synthesis and function of phospholipids in *Staphylococcus aureus*. *Int J Med Microbiol*. 2015; 305(2):196–202. <https://doi.org/10.1016/j.ijmm.2014.12.016> PMID: 25595024.
  46. Mayr JA. Lipid metabolism in mitochondrial membranes. *Journal of inherited metabolic disease*. 2015; 38(1):137–44. <https://doi.org/10.1007/s10545-014-9748-x> PMID: 25082432.
  47. Kubica M, Guzik K, Koziel J, Zarebski M, Richter W, Gajkowska B, et al. A potential new pathway for *Staphylococcus aureus* dissemination: the silent survival of *S. aureus* phagocytosed by human monocyte-derived macrophages. *PloS one*. 2008; 3(1):e1409. <https://doi.org/10.1371/journal.pone.0001409> PMID: 18183290; PubMed Central PMCID: PMC2169301.
  48. Flannagan RS, Heit B, Heinrichs DE. Intracellular replication of *Staphylococcus aureus* in mature phagolysosomes in macrophages precedes host cell death, and bacterial escape and dissemination. *Cellular microbiology*. 2016; 18(4):514–35. <https://doi.org/10.1111/cmi.12527> PMID: 26408990.
  49. Relloso M, Cheng TY, Im JS, Parisini E, Roura-Mir C, DeBono C, et al. pH-dependent interdomain tethers of CD1b regulate its antigen capture. *Immunity*. 2008; 28(6):774–86. <https://doi.org/10.1016/j.immuni.2008.04.017> PMID: 18538591; PubMed Central PMCID: PMC2753602.
  50. Cohen NR, Garg S, Brenner MB. Antigen Presentation by CD1 Lipids, T Cells, and NKT Cells in Microbial Immunity. *Advances in immunology*. 2009; 102:1–94. [https://doi.org/10.1016/S0065-2776\(09\)01201-2](https://doi.org/10.1016/S0065-2776(09)01201-2) PMID: 19477319.
  51. Choi HJ, Xu H, Geng Y, Colmone A, Cho H, Wang CR. Bacterial infection alters the kinetics and function of iNKT cell responses. *Journal of leukocyte biology*. 2008; 84(6):1462–71. <https://doi.org/10.1189/jlb.0108038> PMID: 18772281; PubMed Central PMCID: PMC2614593.
  52. Barin JG, Talor MV, Schaub JA, Diny NL, Hou X, Hoyer M, et al. Collaborative Interferon-gamma and Interleukin-17 Signaling Protects the Oral Mucosa from *Staphylococcus aureus*. *The American journal of pathology*. 2016; 186(9):2337–52. <https://doi.org/10.1016/j.ajpath.2016.07.001> PMID: 27470712; PubMed Central PMCID: PMC5012512.
  53. Sasaki S, Nishikawa S, Miura T, Mizuki M, Yamada K, Madarame H, et al. Interleukin-4 and interleukin-10 are involved in host resistance to *Staphylococcus aureus* infection through regulation of gamma interferon. *Infection and immunity*. 2000; 68(5):2424–30. <https://doi.org/10.1128/iai.68.5.2424-2430.2000> PMID: 10768926; PubMed Central PMCID: PMC97441.
  54. Layre E, Sweet L, Hong S, Madigan CA, Desjardins D, Young DC, et al. A comparative lipidomics platform for chemotaxonomic analysis of *Mycobacterium tuberculosis*. *Chem Biol*. 2011; 18(12):1537–49. <https://doi.org/10.1016/j.chembiol.2011.10.013> PMID: 22195556; PubMed Central PMCID: PMC3407843.
  55. Andra J, Goldmann T, Ernst CM, Peschel A, Gutschmann T. Multiple peptide resistance factor (MprF)-mediated Resistance of *Staphylococcus aureus* against antimicrobial peptides coincides with a

- modulated peptide interaction with artificial membranes comprising lysyl-phosphatidylglycerol. *The Journal of biological chemistry*. 2011; 286(21):18692–700. <https://doi.org/10.1074/jbc.M111.226886> PMID: 21474443; PubMed Central PMCID: PMC3099686.
56. Kilelee E, Pokorny A, Yeaman MR, Bayer AS. Lysyl-phosphatidylglycerol attenuates membrane perturbation rather than surface association of the cationic antimicrobial peptide 6W-RP-1 in a model membrane system: implications for daptomycin resistance. *Antimicrobial agents and chemotherapy*. 2010; 54(10):4476–9. <https://doi.org/10.1128/AAC.00191-10> PMID: 20660664; PubMed Central PMCID: PMC2944598.
  57. Mishra NN, Bayer AS. Correlation of cell membrane lipid profiles with daptomycin resistance in methicillin-resistant *Staphylococcus aureus*. *Antimicrobial agents and chemotherapy*. 2013; 57(2):1082–5. <https://doi.org/10.1128/AAC.02182-12> PMID: 23254419; PubMed Central PMCID: PMC3553710.
  58. Purvis HA, Stoop JN, Mann J, Woods S, Kozijn AE, Hambleton S, et al. Low-strength T-cell activation promotes Th17 responses. *Blood*. 2010; 116(23):4829–37. <https://doi.org/10.1182/blood-2010-03-272153> PMID: 20713963; PubMed Central PMCID: PMC3223073.
  59. Rashid R, Cazenave-Gassiot A, Gao IH, Nair ZJ, Kumar JK, Gao L, et al. Comprehensive analysis of phospholipids and glycolipids in the opportunistic pathogen *Enterococcus faecalis*. *PloS one*. 2017; 12(4):e0175886. <https://doi.org/10.1371/journal.pone.0175886> PMID: 28423018; PubMed Central PMCID: PMC5397010.
  60. de Jong A, Arce EC, Cheng TY, van Summeren RP, Feringa BL, Dudkin V, et al. CD1c presentation of synthetic glycolipid antigens with foreign alkyl branching motifs. *Chem Biol*. 2007; 14(11):1232–42. <https://doi.org/10.1016/j.chembiol.2007.09.010> PMID: 18022562; PubMed Central PMCID: PMC2692252.
  61. Mitchell NJ, Seaton P, Pokorny A. Branched phospholipids render lipid vesicles more susceptible to membrane-active peptides. *Biochimica et biophysica acta*. 2016; 1858(5):988–94. <https://doi.org/10.1016/j.bbamem.2015.10.014> PMID: 26514602; PubMed Central PMCID: PMC4809760.
  62. Fowler VG, Allen KB, Moreira ED, Moustafa M, Isgro F, Boucher HW, et al. Effect of an investigational vaccine for preventing *Staphylococcus aureus* infections after cardiothoracic surgery: a randomized trial. *JAMA*. 2013; 309(13):1368–78. <https://doi.org/10.1001/jama.2013.3010> PMID: 23549582.
  63. Horn J, Stelzner K, Rudel T, Fraunholz M. Inside job: *Staphylococcus aureus* host-pathogen interactions. *International journal of medical microbiology: IJMM*. 2018; 308(6):607–24. <https://doi.org/10.1016/j.ijmm.2017.11.009> PMID: 29217333.
  64. O'Keeffe KM, Wilk MM, Leech JM, Murphy AG, Laabei M, Monk IR, et al. Manipulation of Autophagy in Phagocytes Facilitates *Staphylococcus aureus* Bloodstream Infection. *Infection and immunity*. 2015; 83(9):3445–57. <https://doi.org/10.1128/IAI.00358-15> PMID: 26099586; PubMed Central PMCID: PMC4534639.
  65. Spolski R, West EE, Li P, Veenbergen S, Yung S, Kazemian M, et al. IL-21/type I interferon interplay regulates neutrophil-dependent innate immune responses to *Staphylococcus aureus*. *Elife*. 2019; 8. <https://doi.org/10.7554/eLife.45501> PMID: 30969166; PubMed Central PMCID: PMC6504231.
  66. Commandeur S, Coppola M, Dijkman K, Friggen AH, van Meijgaarden KE, van den Eeden SJ, et al. Clonal analysis of the T-cell response to in vivo expressed *Mycobacterium tuberculosis* protein Rv2034, using a CD154 expression based T-cell cloning method. *PloS one*. 2014; 9(6):e99203. <https://doi.org/10.1371/journal.pone.0099203> PMID: 24905579; PubMed Central PMCID: PMC4048274.
  67. Vorkas CK, Wipperfman MF, Li K, Bean J, Bhattarai SK, Adamow M, et al. Mucosal-associated invariant and  $\gamma\delta$  T cell subsets respond to initial *Mycobacterium tuberculosis* infection. *JCI Insight*. 2018; 3(19). <https://doi.org/10.1172/jci.insight.121899> PMID: 30282828; PubMed Central PMCID: PMC6237486.
  68. Walch M, Dotiwala F, Mulik S, Thiery J, Kirchhausen T, Clayberger C, et al. Cytotoxic cells kill intracellular bacteria through granulysin-mediated delivery of granzymes. *Cell*. 2014; 157(6):1309–23. <https://doi.org/10.1016/j.cell.2014.03.062> PMID: 24906149; PubMed Central PMCID: PMC4090916.
  69. Nakane A, Okamoto M, Asano M, Kohanawa M, Minagawa T. Endogenous gamma interferon, tumor necrosis factor, and interleukin-6 in *Staphylococcus aureus* infection in mice. *Infection and immunity*. 1995; 63(4):1165–72. PMID: 7890367; PubMed Central PMCID: PMC173129.
  70. Dillen CA, Pinsker BL, Marusina AI, Merleev AA, Farber ON, Liu H, et al. Clonally expanded  $\gamma\delta$  T cells protect against *Staphylococcus aureus* skin reinfection. *The Journal of clinical investigation*. 2018; 128(3):1026–42. <https://doi.org/10.1172/JCI96481> PMID: 29400698; PubMed Central PMCID: PMC5824877.
  71. Chen YH, Chiu NM, Mandal M, Wang N, Wang CR. Impaired NK1+ T cell development and early IL-4 production in CD1-deficient mice. *Immunity*. 1997; 6(4):459–67. [https://doi.org/10.1016/s1074-7613\(00\)80289-7](https://doi.org/10.1016/s1074-7613(00)80289-7) PMID: 9133425.

72. DuMont AL, Yoong P, Surewaard BG, Benson MA, Nijland R, van Strijp JA, et al. *Staphylococcus aureus* elaborates leukocidin AB to mediate escape from within human neutrophils. *Infection and immunity*. 2013; 81(5):1830–41. <https://doi.org/10.1128/IAI.00095-13> PMID: 23509138; PubMed Central PMCID: PMC3648020.
73. Zorzoli A, Grayczyk JP, Alonzo F 3rd. *Staphylococcus aureus* Tissue Infection During Sepsis Is Supported by Differential Use of Bacterial or Host-Derived Lipoic Acid. *PLoS pathogens*. 2016; 12(10): e1005933. <https://doi.org/10.1371/journal.ppat.1005933> PMID: 27701474; PubMed Central PMCID: PMC5049849.
74. Chun T, Page MJ, Gapin L, Matsuda JL, Xu H, Nguyen H, et al. CD1d-expressing dendritic cells but not thymic epithelial cells can mediate negative selection of NKT cells. *The Journal of experimental medicine*. 2003; 197(7):907–18. <https://doi.org/10.1084/jem.20021366> PMID: 12682110; PubMed Central PMCID: PMC2193895.
75. Bligh EG, Dyer WJ. A rapid method of total lipid extraction and purification. *Can J Biochem Physiol*. 1959; 37(8):911–7. <https://doi.org/10.1139/o59-099> PMID: 13671378.
76. Vaskovsky VE, Kostetsky EY, Vasendin IM. A universal reagent for phospholipid analysis. *J Chromatogr*. 1975; 114(1):129–41. [https://doi.org/10.1016/s0021-9673\(00\)85249-8](https://doi.org/10.1016/s0021-9673(00)85249-8) PMID: 1237496.
77. Moody DB, Ulrichs T, Muhlecker W, Young DC, Gurcha SS, Grant E, et al. CD1c-mediated T-cell recognition of isoprenoid glycolipids in *Mycobacterium tuberculosis* infection. *Nature*. 2000; 404(6780):884–8. <https://doi.org/10.1038/35009119> PMID: 10786796.
78. Visvabharathy L, Freitag NE. Propofol Sedation Exacerbates Kidney Pathology and Dissemination of Bacteria during *Staphylococcus aureus* Bloodstream Infections. *Infection and immunity*. 2017; 85(7). <https://doi.org/10.1128/IAI.00097-17> PMID: 28461390; PubMed Central PMCID: PMC5478955.